

# Time-dependent corrections to the Ly $\alpha$ escape probability during cosmological recombination

J. Chluba<sup>1</sup> and R. A. Sunyaev<sup>1,2</sup>

<sup>1</sup> Max-Planck-Institut für Astrophysik, Karl-Schwarzschild-Str. 1, 85741 Garching bei München, Germany  
e-mail: jchluba@mpa-garching.mpg.de

<sup>2</sup> Space Research Institute, Russian Academy of Sciences, Profsoyuznaya 84/32, 117997 Moscow, Russia

Received 7 October 2008 / Accepted 10 November 2008

## ABSTRACT

We consider the effects connected with the detailed radiative transfer during the epoch of cosmological recombination on the ionization history of our Universe. We focus on the escape of photons from the hydrogen Lyman  $\alpha$  resonance at redshifts  $600 \lesssim z \lesssim 2000$ , one of two key mechanisms defining the rate of cosmological recombination. We approach this problem within the standard formulation, and corrections due to two-photon interactions are deferred to another paper.

As a main result we show here that within a non-stationary approach to the escape problem, the resulting correction in the free electron fraction,  $N_e$ , is about  $\sim 1.6$ – $1.8\%$  in the redshift range  $800 \lesssim z \lesssim 1200$ . Therefore the discussed process results in one of the largest modifications to the ionization history close to the maximum of Thomson-visibility function at  $z \sim 1100$  considered so far.

We prove our results both numerically and analytically, deriving the escape probability, and considering both Lyman  $\alpha$  line emission and line absorption in a way different from the Sobolev approximation. In particular, we give a detailed derivation of the Sobolev escape probability during hydrogen recombination, and explain the underlying assumptions. We then discuss the escape of photons for the case of coherent scattering in the lab frame, solving this problem analytically in the quasi-stationary approximation and also in the time-dependent case. We show here that during hydrogen recombination the Sobolev approximation for the escape probability is not valid at the level of  $\Delta P/P \sim 5$ – $10\%$ . This is because during recombination the ionization degree changes significantly over a characteristic time  $\Delta z/z \sim 10\%$ , so that at percent level accuracy the photon distribution is not evolving along a sequence of quasi-stationary stages. Non-stationary corrections increase the effective escape by  $\Delta P/P \sim +6.4\%$  at  $z \sim 1490$ , and decrease it by  $\Delta P/P \sim -7.6\%$  close to the maximum of the Thomson-visibility function. We also demonstrate the crucial role of line emission and absorption in distant wings (hundreds and thousands of Doppler widths from the resonance) for this effect, and argue that the final answer probably can only be given within a more rigorous formulation of the problem using a two- or multi-photon description.

**Key words.** radiative transfer – cosmology: cosmic microwave background – cosmology: early Universe – cosmology: theory – atomic processes – cosmology: cosmological parameters

## 1. Introduction

The extraordinary advances in observations of the Cosmic Microwave Background (CMB) temperature and polarization angular anisotropies (e.g. Page et al. 2006; Hinshaw et al. 2006) and the prospects with the PLANCK Surveyor<sup>1</sup> have motivated several groups to re-examine the problem of cosmological recombination (e.g. see Sunyaev & Chluba 2007; Fendt et al. 2008, for detailed overview), including subtle physical processes during hydrogen (e.g. see Dubrovich & Grachev 2005; Chluba & Sunyaev 2006b; Kholupenko & Ivanchik 2006; Rubiño-Martín et al. 2006; Chluba & Sunyaev 2007; Hirata 2008) and helium recombination (e.g. see Switzer & Hirata 2008a,b; Hirata & Switzer 2008; Kholupenko et al. 2007; Wong & Scott 2007; Rubiño-Martín et al. 2008; Kholupenko et al. 2008). It has been argued that percent level corrections to the ionization history exist, which should be taken into account for future determinations of cosmological parameters using CMB data obtained with the PLANCK Surveyor.

In this paper we investigate the validity of one of the key simplifications used for computations of the hydrogen recombination history within existing multi-level recombination

codes: the Sobolev approximation for the escape of Lyman  $\alpha$  photons from the center of the resonance. With this approximation it is possible to separate the problem of the evolution of the photon field and the populations of the hydrogen atom.

Originally the Sobolev approximation was developed in order to describe the escape of photons from finite expanding envelopes of planetary nebulae and stars (Sobolev 1960), but it has been shown that even for cosmological applications, i.e. infinite slowly expanding media, it is very useful (Grachev & Dubrovich 1991; Hummer & Rybicki 1992; Rybicki & dell’Antonio 1994). It gives the same answer as less sophisticated methods, based on simple solutions of the integral or differential equations of radiative transfer, which were used to solve the cosmological hydrogen recombination problem in the 1960s (Varshalovich & Syunyaev 1968; Zeldovich et al. 1968; Peebles 1968). Both for the Sobolev approximation and these simpler derivations the main assumptions are: (i) the properties of the medium (e.g. ionization degree, density, expansion rate) do not change much while the photons interact strongly with the Lyman  $\alpha$  resonance and (ii) each scattering leads to a complete redistribution of photons over the whole line profile.

Due to assumption (i) it is possible to approximate the evolution of the photon distribution as quasi-stationary, which for

<sup>1</sup> [www.rssd.esa.int/Planck](http://www.rssd.esa.int/Planck)

conditions in our Universe seems to be reasonable (Rybicki & dell’Antonio 1994). However, up to what level of accuracy remains a difficult question and deserves further investigations. On the other hand, assumption (ii) is much less justified, since complete redistribution requires some process that *destroys the coherence* in the resonance scattering event. This is usually done by *collisional processes*, which for the conditions in our Universe are extremely inefficient (e.g. see Chluba et al. 2007). We will demonstrate here that for present day experimental requirements, i.e. sub-percent level accuracy in the theoretical predictions of the CMB power spectra at large multipoles  $l$  (e.g. see Seljak et al. 2003), both approximations become insufficient.

In order to understand this problem, it is important that the ionization degree during cosmological hydrogen recombination changes with characteristic time  $\Delta z/z \sim 10\%$ . Also, it is clear that photons, which are released in the distant wings of the Lyman  $\alpha$  line<sup>2</sup>, can in principle travel, scatter, and redshift for a very long time until being reabsorbed. Here it is important to distinguish between *line scattering* events, and *line emission* and *absorption* processes. The former only lead to a redistribution of photons over frequency, but *no* net change in the ionization degree, while the latter (which for example are connected with direct transitions of electrons between the continuum and the 2p state) are able to change the number of Lyman  $\alpha$  photons, and hence the ionization degree. Note that during hydrogen recombination, line absorption occurs with much lower probability ( $\sim 10^{-4}$ – $10^{-3}$ ) than line scattering, so that photons only *die* or disappear effectively rather close to the line center (within a few ten to hundred Doppler widths from the resonance), while in the distant wings they mainly scatter. In addition, every photon that was absorbed (or died) will be replaced by a new photon in a line emission event after a very short time. The profile of this line emission is usually described by a Voigt profile, so that the combination of line absorption followed by a line emission appears to lead to a complete redistribution of photons over the *whole* Lyman  $\alpha$  line profile. However, from the microscopic point of view this is not a scattering event<sup>3</sup>.

As explained in Rybicki & dell’Antonio (1994), in the expanding Universe the redistribution of photons due to Lyman  $\alpha$  resonance scattering is more accurately described by so-called type-II redistribution (Hummer 1962) rather than by complete redistribution. In the former case the photon scatters *coherently in the rest-frame of the atom*, so that the changes in the energies of the photon after the scattering event are related to the motion of the atom. Studying this type of redistribution process in detail is beyond the scope of this paper, but our computations (Chluba & Sunyaev 2009b), in very good agreement with earlier works (e.g. see Rybicki & dell’Antonio 1994), show that in a time-dependent formulation of the problem, including *Doppler broadening*, *atomic recoil* and *stimulated emission*<sup>4</sup>, the actual solution for the scattered photon distribution is very close to the one in the case of *no redistribution*, or equivalently *no line scattering*. Here we show in addition that the assumption of complete redistribution leads to several unphysical conclusions, both in the quasi-stationary approximation and a

time-dependent approach. This is due to the very peculiar conditions in our Universe, where collisional processes are not important, and in particular where due to the low Hubble expansion rate, the Sobolev optical depth reaches extreme values of  $\sim 10^6$ – $10^8$  during recombination.

We therefore investigate the evolution of the photon field in the no-scattering approximation and show that time-dependent corrections to the effective escape probability are important at the level of  $\sim 5\%$ – $10\%$  (see Sect. 3.4, Figs. 5 and 8). As mentioned above, this is due to the fact that in the distant wings of the Lyman  $\alpha$  resonance photons mainly scatter, but do not disappear. This renders it important to include changes in the ionization degree and photon emission rate during the evolution of the photon field in the computations, implying that the quasi-stationary approximation becomes inaccurate. Both changes in the absorption optical depth and the effective emission rate cannot be neglected. The corresponding time-dependent changes in the free electron fraction, which are important for the Thomson visibility function and in computations of the CMB power spectra, reach the level of  $\sim 1.6$ – $1.8\%$  in the redshift range  $800 \lesssim z \lesssim 1200$  (see Sect. 4 and Fig. 12), and therefore are about 2 times as large as those due to atomic recoil, recently studied by Grachev & Dubrovich (2008). Taking the time-dependent correction investigated here into account will therefore be very important for the analysis of future CMB data from the PLANCK Surveyor.

We also briefly discuss another aspect of the Sobolev approximation, which is connected to the *shape* of the Lyman  $\alpha$  line profile (see Sect. 3.5). In the Sobolev approximation there is no direct dependence of the Sobolev escape probability on the shape of the line emission, absorption, and scattering profiles, as long as all are *identical*. Our derivation also clearly shows this point (cf. Sects. 3.2 and 3.5). Therefore, in principle it does not matter if the profile is assumed to be a Lorentzian, a Voigt profile, a pure Doppler profile, or a  $\delta$  function. It also turns out that in the no line scattering approximation this is true, as long as the line emission and absorption profiles are identical, and the evolution of the photon distribution is quasi-stationary (cf. Sects. 3.3 and 3.5).

However, if one includes the deviations from quasi-stationarity, then the result does depend in detail on the Lyman  $\alpha$  profile, even if the line emission and absorption profiles still are the same. For example, in the case of a pure Doppler profile (very narrow), the problem of the Lyman  $\alpha$  photon escape from the resonance due to the expansion of the Universe would be practically quasi-stationary, and the Sobolev approximation should be applicable. This is because the number of photons emitted and absorbed in the optically thin region of the Lyman  $\alpha$  line is exponentially small, and all the transfer is happening inside the Doppler core, corresponding to  $\Delta\nu/\nu \sim \text{few} \times 10^{-5}$ .

On the other hand in the real problem, Lyman  $\alpha$  emission and absorption also occurs in the distant Lorentz wings (at hundreds and thousands of Doppler widths) of the resonance. As we show here, at a percent level the number of these photons is very important for the value of the effective escape probability (e.g. see Fig. 10). This shows that it is crucial to understand the profiles (or cross-sections) of the considered processes in more detail, and for this probably a formulation in the two- or multi-photon picture will become necessary. Also in principle it should be possible to distinguish between different redistribution processes for the line scattering event, by measuring the shape and position of the residual, present day CMB Lyman  $\alpha$  distortion.

It is extremely impressive that the standard estimates of the Lyman  $\alpha$  escape probability, which were used in the first papers on cosmological recombination, and the Sobolev approximation

<sup>2</sup> At redshift  $z = 1100$  a thousand Doppler width corresponds to  $\Delta\nu/\nu \sim 2\%$ , a distance from the line center that can be passed by redshifting in  $\Delta z/z \sim 2\%$ .

<sup>3</sup> Switzer & Hirata (2008a) also make this distinction using the termini of incoherent processes and coherent scattering.

<sup>4</sup> Within a Fokker-Planck approach the atomic recoil effect was first included by Basko (1978), while the effect of stimulated emission was only taken into account very recently by Rybicki (2006).

give such precise (better than 5–10%) answers, even though they are based on two incorrect assumptions as mentioned above. It is well known that the principal difference (from a physical point of view) between the cases of partial and complete redistribution does not influence the final result very much in the majority of astrophysical applications (Ivanov 1973). However, the enormous requirements of accuracy of theoretical estimates in the era of precise cosmology change the situation, and force us to search for percent level corrections to the escape of Ly  $\alpha$  photons from resonance during the epoch of cosmological recombination.

## 2. Transfer equations for the photon field

In this section we provide the transfer equation describing the evolution of the photon distribution in the vicinity of the Lyman  $\alpha$  resonance. We include the effect of *line emission* and *line absorption* in the expanding Universe for the cases of *coherent line scattering* in the lab frame, and *complete redistribution*. Here we envision all processes as 1 + 1 photon processes, as in the Seaton-cascade description (Seaton 1959), but leave the treatment of correction due to two-photon interactions for a future paper. Also the effects of partial frequency redistribution will be discussed in separate paper. In Sects. 2.3 and 2.4 we give the time-dependent solutions of these equations. We will use these results in Sect. 3 to deduce the Lyman  $\alpha$  escape probability, which then can be utilized to estimate the corrections to the cosmological ionization history.

### 2.1. General kinetic equation for the photon field

To follow the evolution of the photon field in the expanding Universe we start with the kinetic equation for the function  $N_\nu = I_\nu/h\nu$ , where  $I_\nu$  is the *physical* specific intensity of the isotropic, ambient radiation field (e.g. see Rybicki & dell'Antonio 1994):

$$\frac{1}{c} \left[ \frac{\partial N_\nu}{\partial t} \Big|_\nu + 2HN_\nu - H\nu \frac{\partial N_\nu}{\partial \nu} \Big|_\nu \right] = C[N_\nu]. \quad (1)$$

Here  $H(z)$  is the Hubble parameter as a function of redshift  $z$  and  $C[N_\nu]$  is the collision term, which describes the emission, absorption and frequency redistribution processes.

In order to simplify the left hand side of the Eq. (1) we transform to the frequency variable  $x = \nu/(1+z)$ , so that

$$N_\nu = \frac{dx}{d\nu} N_x = \frac{N_x}{(1+z)}. \quad (2)$$

Inserting this into Eq. (1) yields

$$\frac{1}{c} \left[ \frac{\partial N_x}{\partial t} \Big|_x + 3HN_x - Hx \frac{\partial N_x}{\partial x} \Big|_x \right] = (1+z)C[N_\nu]. \quad (3)$$

To obtain  $dN_x/dt|_x$  one can use the total differential of  $N_x$

$$dN_x = \frac{\partial N_x}{\partial t} \Big|_x dt + \frac{\partial N_x}{\partial x} \Big|_x dx \quad (4)$$

which with  $dx/dt|_x = xH$  then gives

$$\frac{\partial N_x}{\partial t} \Big|_x = \frac{\partial N_x}{\partial t} \Big|_x + Hx \frac{\partial N_x}{\partial x} \Big|_x. \quad (5)$$

Inserting this into Eq. (3) one finds

$$\frac{1}{c} \left[ \frac{\partial N_x}{\partial t} \Big|_x + 3HN_x \right] = (1+z)C[N_\nu]. \quad (6)$$

Here the redshifting term was absorbed due to the choice of the frequency variable.

The term  $3HN_x$  can be eliminated using the substitution  $\tilde{N}_x = N_x/(1+z)^3 \equiv N_\nu/(1+z)^2$ , so that Eq. (1) takes the form

$$\frac{1}{c} \frac{\partial \tilde{N}_x}{\partial t} \Big|_x = \frac{C[N_\nu]}{(1+z)^2}. \quad (7)$$

One can easily verify that in the absence of physical interactions ( $C[N_\nu] \equiv 0$ ), in spite of the Hubble expansion, a Planckian spectrum is not modified (e.g. see Padmanabhan 2002), so that it is always possible to directly write

$$\frac{1}{c} \frac{\partial \tilde{N}_x}{\partial t} \Big|_x \equiv \frac{1}{c} \frac{\partial \Delta \tilde{N}_x}{\partial t} \Big|_x, \quad (8)$$

where  $\Delta \tilde{N}_x = \tilde{N}_x - \tilde{N}_x^{\text{pl}}$  is the corresponding deviation of the spectrum from a blackbody, which in our coordinates reads

$$\tilde{N}_x^{\text{pl}} = \frac{2}{c^2} \frac{x^2}{e^{hx/kT_0} - 1}. \quad (9)$$

Here  $T_0 = 2.725$  K is the CMB temperature today (Fixsen & Mather 2002).

### 2.2. Line emission and line absorption

Although for conditions in the Universe during cosmological recombination<sup>5</sup> the resonant scattering optical depth close to the Lyman  $\alpha$  line center exceeds unity by several orders of magnitude, only *real* line emission and absorption lead to a *net* change of the photon number. If we consider an electron in the ground state of hydrogen which after the absorption of a photon (say close to the Lyman  $\alpha$  resonance) is excited to the 2p state, then there are two routes out of this level: (i) it can directly decay back to the ground state, re-emitting a photon with (slightly) changed frequency, depending on the considered redistribution process, or (ii) it can be further excited to the *continuum* or *higher shells* ( $n > 2$ ) by the subsequent absorption of a blackbody photon from the CMB. Only in case (ii) does the number of Lyman  $\alpha$  photons really change, while for (i) the photon simply was scattered.

To describe this aspect of the problem, we use the *death probability* or *single scattering albedo*,  $p_d$ , which specifies what fraction of photons that interact with a hydrogen atom in the 1s state, will really disappear from the photon distribution. The scattering probability,  $p_{\text{sc}} = 1 - p_d$ , will then give the fraction of photons that reappear at a different frequency, and hence only underwent a scattering rather than a real line absorption.

#### 2.2.1. Death probability or single scattering albedo

Including all possible ways in and out of the 2p level, the net change in the number density of electrons in the 2p level can be written as

$$\frac{dN_{2p}}{dt} + 3HN_{2p} = \frac{dN_{2p}}{dt} \Big|_{2p}^{\text{Ly}-\alpha} + R_{2p}^+ - R_{2p}^- N_{2p}, \quad (10)$$

<sup>5</sup> Electron and proton collisions are negligible in comparison with radiative processes, like photorecombination or photoionization, and bound-bound dipole transitions (e.g. see Chluba & Sunyaev 2008).

where  $\frac{dN_{2p}}{dt}\Big|_{2p}^{\text{Ly}-\alpha}$  denotes the contribution from the Lyman  $\alpha$  transition, which we will specify below (see Sect. 3.1), and

$$R_{2p}^- = R_{2pc} + \sum_{i>2p} \frac{g_i}{g_{2p}} A_{i2p} n^{\text{pl}}(\nu_{i2p}) \quad (11a)$$

$$R_{2p}^+ = N_e N_p R_{c2p} + \sum_{i>2p} N_i A_{i2p} [1 + n^{\text{pl}}(\nu_{i2p})]. \quad (11b)$$

Here  $N_e$  and  $N_p$  are the electron and proton number densities, and  $n^{\text{pl}} = 1/(e^{h\nu/kT_\gamma} - 1)$  is the blackbody photon occupation number, where  $T_\gamma = T_0(1+z)$  is the CMB temperature at redshift  $z$ . Furthermore,  $A_{i2p}$  denotes the spontaneous dipole transition rate from level  $i$  to the 2p state,  $\nu_{i2p}$  the corresponding transition frequency, and  $g_i$  the statistical weight of level  $i$ .  $R_{c2p}$  and  $R_{2pc}$  are the photorecombination and photoionization coefficients of the 2p state, which are computed assuming that the ambient radiation field is Planckian. Since except for the Lyman series and the 2s-1s two-photon transition, the emission of photons during cosmological hydrogen recombination only produces tiny deviations of the photon distribution from a blackbody spectrum  $B_\nu$  (e.g. see Chluba & Sunyaev 2006a), this approximation is possible. Similarly, we have neglected the spectral distortion in the terms due to transitions from and to higher levels ( $A_{i2p} n_\nu \approx A_{i2p} n_\nu^{\text{pl}}$ ), so that  $R_{2p}^-$  becomes completely independent of the solution for the photon field. However, note that  $R_{2p}^+$  still depends on the solution for the populations,  $N_i$ , of the excited levels, and the electron and proton number density.

Omitting electron and proton collisions, the total probability for Lyman  $\alpha$  emission  $p_{\text{em}}$  is therefore given by

$$p_{\text{em}} = \frac{A_{21}}{A_{21} + R_{2p}^-}, \quad (12)$$

where  $A_{21} = 6.27 \times 10^8 \text{ s}^{-1}$  is the spontaneous 2p-1s transition rate. The corresponding probability for the *death* of photons, i.e. removal of Lyman  $\alpha$  photons or return of 2p electrons to the continuum or higher levels, is then given by  $p_d = 1 - p_{\text{em}}$ .

Note that in Eq. (12) we directly neglected the effects of stimulated emission. This approximation is well justified, since close to the Lyman  $\alpha$  transition the photon occupation number  $n_\nu = \frac{c^2 I_\nu}{2h\nu^3} \ll 1$  at all relevant redshifts.

In Fig. 1 we show the death probability,  $p_d$ , as a function of redshift considering a 2, 3 and 10 shell hydrogen atom. It is clear that the largest contribution to the death probability comes from the third shell, and cases with  $n \geq 3$  are practically indistinguishable. This is because during cosmological hydrogen recombination  $R_{2pc} \ll \frac{1}{3}[A_{3s2p} + 5A_{3d2p}] n^{\text{pl}}(\nu_{3s2p})$ , and since  $n^{\text{pl}}(\nu_{3s2p})$ , for  $n > 3$ , is exponentially larger than  $n^{\text{pl}}(\nu_{ns2p})$ , so that also  $[A_{3s2p} + 5A_{3d2p}] n^{\text{pl}}(\nu_{3s2p}) \gg [A_{ns2p} + 5A_{nd2p}] n^{\text{pl}}(\nu_{ns2p})$ . This fact implies that for a consistent investigation of the Lyman  $\alpha$  escape problem, one should include at least 3 shells in the computations.

### 2.2.2. Line emission profile

The form of the emission profile for the Lyman  $\alpha$  line (under the assumption of complete redistribution) is known from quantum-mechanical considerations. Including the thermal motion of the hydrogen atoms it is usually described using the so-called *Voigt* profile:

$$\varphi(\nu) = \frac{a}{\pi^{3/2} \Delta\nu_D} \int_{-\infty}^{\infty} \frac{e^{-t^2} dt}{a^2 + (x_D - t)^2} = \frac{\phi(\nu)}{\Delta\nu_D}, \quad (13a)$$

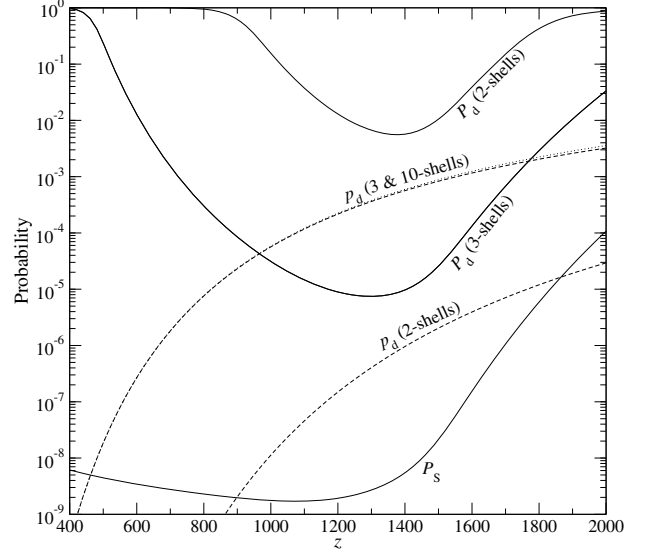


**Fig. 1.** Different probabilities for the cosmological hydrogen recombination problem as a function of redshift. The death probabilities,  $p_d$ , for a 2, 3 (dashed lines), and 10 shell hydrogen atom (dotted line) are shown. The death probability for the 3 shell case already practically coincides with the death probability for the 10 shell case. The solid lines show different escape probabilities.  $P_s = [1 - e^{-\tau_s}]/\tau_s$  denotes the normal Sobolev escape probability, while  $P_d = [1 - e^{-\tau_d}]/\tau_d$ , where  $\tau_d = p_d \tau_s$ . To compute  $\tau_s$  we used the RECFAST solution for  $N_{1s}$ .

where for the H I Lyman  $\alpha$  transition the Voigt parameter,  $a$ , the Doppler width of the line due to the thermal motion of the hydrogen atoms,  $\Delta\nu_D$ , and the variable  $x_D$  are defined by

$$a = \frac{A_{21}}{4\pi\Delta\nu_D} \approx 8.61 \times 10^{-4} \left[ \frac{(1+z)}{1100\chi} \right]^{-1/2} \quad (13b)$$

$$\frac{\Delta\nu_D}{\nu_{21}} = \sqrt{\frac{2k_B T_e}{m_{\text{H}} c^2}} \approx 2.35 \times 10^{-5} \left[ \frac{(1+z)}{1100\chi} \right]^{1/2} \quad (13c)$$

$$x_D = \frac{\nu - \nu_{21}}{\Delta\nu_D}. \quad (13d)$$

Here  $\nu_{21} \approx 2.47 \times 10^{15} \text{ Hz}$  is the Lyman  $\alpha$  transition frequency and  $\chi = T_\gamma/T_e$ .

The Voigt profile is normalized such that  $\int_0^\infty \frac{\varphi(\nu)}{4\pi} d\nu d\Omega \equiv 1$  and it has the well known limiting cases

$$\phi(\nu) \approx \begin{cases} \frac{a}{\pi x_D} & \text{for } |x_D| \gtrsim 10 \\ \mathcal{N} \frac{e^{-x_D^2}}{\sqrt{\pi}} & \text{for } x_D \sim 0 \end{cases}, \quad (14)$$

with  $\mathcal{N} = e^{a^2} \text{Erfc}(a) \approx 1 - 2a/\sqrt{\pi} + a^2$  for  $a \ll 1$  and where  $\text{Erfc}(x)$  denotes the complementary error function.

In addition, on the red side of the resonance one can approximate the integral  $\chi = \int_0^\infty \phi(\nu') d\nu'$  by

$$\chi_{\text{wings}} \approx 2.73 \times 10^{-6} \left[ \frac{(1+z)}{1100\chi} \right]^{-1/2} \left[ \frac{x_D}{-100} \right]^{-1}, \quad (15)$$

as long as  $-\nu_{21}/\Delta\nu_D \ll x_D \lesssim -10$ . This formula shows that only a very small fraction of photons is directly emitted in the distant wings. However it is also known that escape of photons from the Doppler core is extremely strongly suppressed. As a result the emission of the photons in the distant wings should be considered carefully.

### 2.2.3. Line emission term

With the definitions given above, the term for real emission of photons due the addition of *fresh electrons* to the 2p state can be written as

$$\frac{1}{c} \frac{dN_\nu}{dt} \Big|_{\text{Ly-}\alpha}^{\text{em}} = p_{\text{em}} \frac{\phi(\nu)}{4\pi \Delta\nu_D} \times R_{2p}^+. \quad (16)$$

The emission probability,  $p_{\text{em}}$ , is defined in Eq. (12). Again we have neglected the factors related to stimulated emission.

For Eq. (16) we have assumed that the emission profile for every new electron that was added to the 2p state is given by Eq. (13), regardless of whether the electron came from the continuum or from some excited state. In the absence of collisions (a very good approximation for the expanding Universe) this is the standard approach, in which fresh electrons, i.e. those that have *not* reached the 2p state by a line scattering event, lead to a *natural excitation* of the 2p state (e.g. see p. 433 Mihalas 1978). Note that this also implicitly means that any transition of electrons from the 2p state to higher levels effectively leads to a complete redistribution of photons in the Lyman  $\alpha$  line.

One does expect some corrections related to these approximations, since even for the real line emission process the history of the electron should matter (e.g. due to two-photon processes Chluba & Sunyaev 2008). However, this problem is beyond the scope of this paper.

### 2.2.4. Line absorption term

In the standard formulation (e.g. see Mihalas 1978, p. 278) the profile for real line absorption is usually assumed to have the same shape as the natural emission profile 13. In this case, using the death probability  $p_d$ , the term for real line absorption reads

$$\frac{1}{c} \frac{dN_\nu}{dt} \Big|_{\text{Ly-}\alpha}^{\text{abs}} = p_d h\nu_{21} B_{12} N_{1s} \frac{\phi(\nu)}{4\pi \Delta\nu_D} N_\nu. \quad (17)$$

Here  $N_{1s}$  is the number density of hydrogen atoms in the ground state, and  $B_{12}$  is the Einstein coefficient for Lyman  $\alpha$  absorption. The idea behind Eq. (17) is that only a fraction  $p_d$  of the photons interacting with the Lyman  $\alpha$  line really undergo transitions to higher levels or the continuum, while most of the interactions ( $p_{\text{sc}} \equiv p_{\text{em}} = 1 - p_d$ ) actually should be considered as *resonance scattering* events.

More rigorously, using the principle of detailed balance, instead of the standard absorption coefficient  $\alpha_\nu^{\text{st}} = h\nu_{21} B_{12} N_{1s} \frac{\phi(\nu)}{4\pi \Delta\nu_D}$  (e.g. see Mihalas 1978, p. 78), from Eq. (16), also including the effect of stimulated emission, one would deduce  $\alpha_\nu = \frac{\nu_{21}^3}{\nu^2} e^{h[\nu-\nu_{21}]/kT_\gamma} \times \alpha_\nu^{\text{st}}$ . Although especially the exponential term should lead to significant differences in the distant wings of the Lyman  $\alpha$  line, we follow the standard approximation and set  $\frac{\nu_{21}^3}{\nu^2} e^{h[\nu-\nu_{21}]/kT_\gamma} \sim 1$  in this expression.

It is clear that in the distant wings other corrections also will become very important (e.g. due to two-photon emission Chluba & Sunyaev 2008), but a full consideration of these aspects is beyond the scope of this paper. However, in the standard formulation, i.e. setting  $\frac{\nu_{21}^3}{\nu^2} e^{h[\nu-\nu_{21}]/kT_\gamma} \sim 1$ , already at  $|x_D| \gtrsim 100\text{--}1000$  a blackbody distribution is not exactly conserved in full equilibrium. At the level of accuracy required in the cosmological recombination problem this aspect will have to be resolved.

### 2.2.5. Final line emission and absorption term

With Eqs. (16) and (17) one can now write down the collision term for real line emission and absorption as

$$\begin{aligned} C[N_\nu]_{\text{e/a}} &= p_{\text{em}} \frac{\phi(\nu)}{4\pi \Delta\nu_D} R_{2p}^+ - p_d \sigma_r N_{1s} \phi N_\nu \\ &= p_d \sigma_r N_{1s} \phi(\nu) \{N_{\text{em}} - N_\nu\} \end{aligned} \quad (18a)$$

$$N_{\text{em}} = \frac{p_{\text{em}}}{p_d} \frac{R_{2p}^+}{h\nu_{21} B_{12} N_{1s}} = \frac{2\nu_{21}^2}{c^2} \frac{g_{1s}}{g_{2p}} \frac{R_{2p}^+}{R_{2p}^- N_{1s}}. \quad (18b)$$

Here we used the resonant scattering cross section

$$\begin{aligned} \sigma_r &= \frac{h\nu_{21}}{4\pi} \frac{B_{12}}{\Delta\nu_D} \equiv \frac{\pi e^2}{m_e c} \frac{f_{12}}{\Delta\nu_D} \equiv \frac{3\lambda_{21}^2 a}{2} \\ &\approx 1.91 \times 10^{-13} \text{cm}^2 \left[ \frac{(1+z)}{1100\chi} \right]^{-1/2}, \end{aligned} \quad (19)$$

and the Einstein relations  $A_{21} = \frac{2h\nu_{21}^3}{c^2} B_{21}$  and  $B_{21} = \frac{g_{1s}}{g_{2p}} B_{12}$ , where  $\lambda_{21} = c/\nu_{21}$  is the Lyman  $\alpha$  wavelength, and  $f_{12}$  is the absorption oscillator strength of the Lyman  $\alpha$  transition. Note that  $N_{\text{em}}$  is only a function of redshift, but not frequency. Furthermore, due to the factor  $R_{2p}^+$  it depends on the solution for the population of the higher levels.

### 2.3. Transfer equation including line emission, line absorption and coherent scattering in the lab frame

For coherent scattering in the lab frame no redistribution of photons over frequency occurs. Using Eqs. (7) and (18), the time-dependent transfer equation therefore reads

$$\frac{1}{c} \frac{\partial \tilde{N}_x}{\partial t} \Big|_x = p_d \sigma_r N_{1s} \phi(\nu) \{ \tilde{N}_{\text{em}} - \tilde{N}_x \}, \quad (20)$$

with  $\nu = x(1+z)$ , and  $\tilde{N}_{\text{em}} = N_{\text{em}}/(1+z)^2$ , where  $N_{\text{em}}$  is defined by Eq. (18b). For the initial condition  $\tilde{N}_x(z_s) = \tilde{N}_x^{\text{pl}}$ , where  $z_s$  is a redshift well before the epoch of hydrogen cosmological recombination, this equation formally has the simple solution

$$\tilde{N}_x(z) = \tilde{N}_x^{\text{pl}} - \int_{z_s}^z [\tilde{N}_{\text{em}}(z') - \tilde{N}_x^{\text{pl}}] \partial_{z'} e^{-\tau_{\text{abs}}(x, z', z)} dz'. \quad (21)$$

Here  $\tau_{\text{abs}}(x, z', z)$  is defined by

$$\tau_{\text{abs}}(x, z', z) = \int_z^{z'} p_d \frac{c \sigma_r N_{1s}}{H(1+\tilde{z})} \phi(x[1+\tilde{z}]) d\tilde{z} \quad (22a)$$

$$= \int_\nu^{\nu'} p_d \frac{c \sigma_r N_{1s}}{H} \phi(\tilde{\nu}) \frac{d\tilde{\nu}}{\tilde{\nu}}. \quad (22b)$$

In Eq. (22b) we have used the substitution  $\tilde{\nu} = x(1+\tilde{z})$ , so that the current redshift can be found from  $1+\tilde{z} = \tilde{\nu}(1+z)/\nu$ . Note that in the given set of variables  $\tilde{N}_x^{\text{pl}}$  does not explicitly depend on redshift, so we omitted it in the notation.

Returning to physical coordinates one can finally write

$$\Delta N_\nu^{\text{coh}}(z) = [N_{\text{em}}(z) - N_{\nu_{21}}^{\text{pl}}(z)] \int_{z_s}^z \Theta^{\text{coh}}(z') \partial_{z'} e^{-\tau_{\text{abs}}(\nu, z', z)} dz', \quad (23a)$$

$$\Theta^{\text{coh}}(z') = \frac{\tilde{N}_{\text{em}}(z') - \tilde{N}_x^{\text{pl}}}{\tilde{N}_{\text{em}}(z) - \tilde{N}_{x_{21}}^{\text{pl}}} \quad (23b)$$

where  $x_{21} = \nu_{21}/(1+z)$  and in expression (22) for  $\tau_{\text{abs}}$  one should use  $x = \nu/(1+z)$ .

### 2.4. Transfer equation including line emission, line absorption and complete redistribution

In the case of complete redistribution one has to add the term (see e.g. Mihalas 1978)

$$C[N_\nu]_r \approx p_{sc} \sigma_r N_{1s} \phi(\nu) [\bar{N} - N_\nu] \quad (24)$$

to Eq. (20). Here  $\bar{N} = \int \frac{\varphi(\nu)}{4\pi} N_\nu d\nu d\Omega$ . This then yields

$$\frac{1}{c} \frac{\partial \tilde{N}_x}{\partial t} \Big|_x = \sigma_r N_{1s} \phi(\nu) \{ \tilde{N}_{em}^{cr} - \tilde{N}_x \}, \quad (25)$$

with  $\tilde{N}_{em}^{cr} = p_d \tilde{N}_{em} + p_{sc} \tilde{N}$ , and  $\tilde{N} = \bar{N}/(1+z)^2$ . Although complete redistribution is not appropriate for conditions valid in the expanding Universe (practically no collisions), it is used many times in the literature, in particular for the derivation of the Sobolev escape probability. One should mention that in this approach it is assumed that even those photons scattering in the very distant red wing of the Lyman  $\alpha$  resonance can directly return to the line center in one scattering event. With Doppler redistribution, which is described by so-call type-II redistribution (Hummer 1962), this is only possible after many scatterings (if at all), or by a real line absorption event.

Comparing Eq. (25) with Eq. (20), in physical coordinates one can directly write down the solution as

$$\Delta N_\nu^{cr}(z) = [N_{em}^{cr}(z) - N_{\nu_{21}}^{pl}(z)] \int_{z_s}^z \Theta^{cr}(z') \partial_{z'} e^{-\tau_{cr}(\nu, z', z)} dz', \quad (26a)$$

$$\Theta^{cr}(z') = \frac{\tilde{N}_{em}^{cr}(z') - \tilde{N}_x^{pl}}{\tilde{N}_{em}^{cr}(z) - \tilde{N}_{x_{21}}^{pl}} \quad (26b)$$

where  $\tau_{cr} \equiv \tau_{abs}|_{p_d=1}$ . It is clear that  $\tau_{cr} \gg \tau_{abs}$  since  $p_d \ll 1$  during cosmological recombination (see Fig. 1).

## 3. The Lyman $\alpha$ escape problem and results for the escape probabilities

In order to solve the cosmological recombination problem, the usual way is to separate the evolution of the photon field from the evolution of the matter, in particular the populations of the different energy states inside the hydrogen atom. This is normally achieved using the Sobolev approximation for the optically thick Lyman series in order to define the mean intensity of photons supporting the  $np$ -state at a given time, and leads to the definition of the *Sobolev escape probability*. In this section we explain the details of this approximation and compare it with other cases that can be solved analytically.

### 3.1. The Lyman $\alpha$ net rate

The net change of the number density of electrons in the 2p level via the Lyman  $\alpha$  channel is given by

$$\begin{aligned} \frac{dN_{2p}}{dt} \Big|_{Ly-\alpha} &= A_{21} \frac{g_{2p}}{g_{1s}} N_{1s} \bar{n} - A_{21} (1 + \bar{n}) N_{2p} \\ &= A_{21} (1 + \bar{n}) N_{2p} \left[ \frac{g_{2p}}{g_{1s}} \frac{N_{1s}}{N_{2p}} \frac{\bar{n}}{1 + \bar{n}} - 1 \right] \end{aligned} \quad (27)$$

where  $A_{21} = 6.27 \times 10^8 \text{ s}^{-1}$  is the spontaneous 2p-1s transition rate,  $N_i$  denotes the number density of electrons in level  $i$ .

Furthermore we made use of the Einstein relations, and defined  $\bar{n} = \frac{c^2 J}{2h\nu_{21}^3}$  with

$$J = \int_0^\infty \frac{\varphi(\nu)}{4\pi} I_\nu d\nu d\Omega. \quad (28)$$

According to the textbook derivations<sup>6</sup>  $J \approx J(\nu_{21}) \approx h\nu_{21} \bar{N} \approx h\nu_{21} \int \frac{\varphi(\nu)}{4\pi} N_\nu d\nu d\Omega \approx \frac{2h\nu_{21}^3}{c^2} \bar{n}$  with very high accuracy, since  $\varphi(\nu)$  is so sharply peaked at  $\nu \approx \nu_{21}$ .

Defining the *line occupation number*

$$n_L = \frac{1}{\frac{g_{2p}}{g_{1s}} \frac{N_{1s}}{N_{2p}} - 1} \approx \frac{g_{1s}}{g_{2p}} \frac{N_{2p}}{N_{1s}} \quad (29)$$

Eq. (27) can be cast into the form

$$\frac{dN_{2p}}{dt} \Big|_{Ly-\alpha} \approx A_{21} \frac{g_{2p}}{g_{1s}} N_{1s} \Delta \bar{n}^L, \quad (30)$$

where we have introduced  $\Delta \bar{n}^L = \bar{n} - n_L$ , for which we will now discuss different approximations below.

### 3.2. Escape probability within the Sobolev approximation

The aim is now to determine the solution for the mean occupation number in the Lyman  $\alpha$  resonance using the Sobolev approximation. The two key assumptions for its derivation are (i) *quasi-stationary* evolution of the photon field and (ii) that every resonance scattering leads to a *complete redistribution* of photons over the whole Lyman  $\alpha$  line profile. With these assumptions we can obtain the solution for the spectral distortion at redshift  $z$  using the results of Sect. 2.4. Under quasi-stationary conditions one can simply set<sup>7</sup>  $\Theta^{cr}(z') = 1$  in Eq. (26), and for the absorption optical depth,  $\tau_{cr}$ , one has

$$\tau_{cr}^{qs}(\nu, z', z) \approx \tau_S(z) \int_{\nu'}^{\nu} \varphi(\tilde{\nu}) d\tilde{\nu}, \quad (31)$$

where  $\varphi(\nu) = \varphi(\nu, z)$  is given by Eq. (13), and  $\nu' = \nu \frac{1+z'}{1+z}$ . Furthermore we introduced the *Sobolev* optical depth of the Lyman  $\alpha$  line

$$\tau_S = \frac{c \sigma_r N_{1s}}{H} \frac{\Delta\nu_D}{\nu_{21}} = \frac{g_{2p}}{g_{1s}} \frac{A_{21} \lambda_{21}^3}{8\pi H} N_{1s} \quad (32)$$

with wavelength  $\lambda_{21} = c/\nu_{21}$ . For Eq. (31) we have assumed that  $\tau_S$  does not change significantly between  $z'$  and  $z$ . Also we have neglected the variation of  $1/\tilde{\nu}$  in comparison with  $\varphi(\nu)$ , and set  $1/\tilde{\nu} \approx 1/\nu_{21}$ . This approximation is normally applied in the literature and computation of the recombination history.

From Eq. (26) with  $\Theta^{cr} = 1$  one then obtains

$$\Delta N_\nu^{cr,qs}(z) = [N_{em}^{cr} - N_{\nu_{21}}^{pl}] [1 - e^{-\tau_S} e^{\tau_S \chi}], \quad (33)$$

with  $\chi(\nu) = \int_0^\nu \varphi(\nu') d\nu'$ .

#### 3.2.1. Spectral characteristics of the solution

As can be seen in Fig. 2, during hydrogen recombination  $\tau_S \gg 1$ . According to Eq. (33) the photon distribution therefore varies strongly close to<sup>8</sup>  $\tau_S [1 - \chi] \sim \ln 2$ , while it is basically identical

<sup>6</sup> Also in the derivation of the Einstein relations this approximation is normally applied.

<sup>7</sup> In fact this approximation not only implies quasi-stationarity, i.e.  $\tilde{N}_{em}^{cr}(z') = \tilde{N}_{em}^{cr}(z)$ , but also that one can use  $\tilde{N}_x^{pl} \approx \tilde{N}_{x_{21}}^{pl}$ .

<sup>8</sup> There the value of  $\Delta N_\nu^{cr,qs}(z)$  has decreased by a factor of 2 compared to the line center.

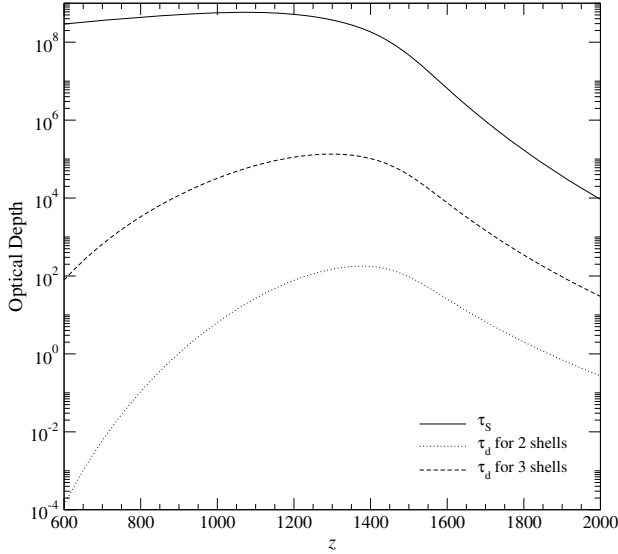


**Fig. 2.** Comparison of the Sobolev optical depth,  $\tau_s$ , as defined by Eq. (32), and the total absorption optical depth,  $\tau_d = p_d \tau_s$ , for the 2- and 3 shell case. To compute  $\tau_s$  we used the RECFAST solution for  $N_{1s}$ .

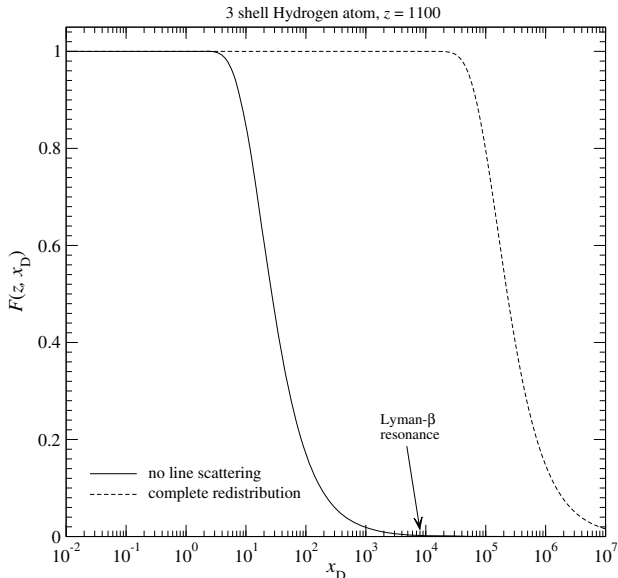


**Fig. 3.** Spectral behavior of the solutions in the quasi-stationary approximation at redshift  $z = 1100$ . We normalized the distortion to unity at the Lyman  $\alpha$  frequency, i.e.  $F \equiv \Delta N_\nu(z)/\Delta N_{\nu_{21}}(z)$ . The solid line shows the result obtained in the no line scattering approximation, while the dashed line represents the solution for the complete redistribution case. We also indicated the position of the Lyman  $\beta$  resonance at that time.

to unity<sup>9</sup> at  $x_D \leq 0$ . Using the wing-expansion (A.2) of the Voigt profile one therefore finds that this happens at a distance of about

$$x_D \approx \frac{a}{\pi} \frac{\tau_S}{\ln 2}. \quad (34)$$

At  $z \sim 1100$  one has  $a \sim 8.6 \times 10^{-4}$  and  $\tau_S \sim 5.8 \times 10^8$ , such that  $x_D \sim 2.3 \times 10^5$ . This shows that in the complete redistribution approximation the photon distribution is in full equilibrium with the value at the line center up to extremely large distances on the blue side of the line center (see Fig. 3).

Physically this type of redistribution does not describe the problem very accurately, and a much more realistic solution is

<sup>9</sup> With relative accuracy better than  $\sim e^{-\tau_S/2}$ .

obtained using the case of coherent scattering in the lab frame (see Sect. 3.3). For example, if we consider the position of the Lyman  $\beta$  line at redshift  $z = 1100$ , then in Doppler units of the Lyman  $\alpha$  line one finds  $x_D^{\text{Ly}\beta} \sim 8000$ . The variation of the photon distribution, which is important for the value of the escape probability (see below), occurs far beyond this value. In fact,  $x_D \sim 2.3 \times 10^5$  corresponds to about 2 times the Lyman  $\alpha$  frequency, or 1.5 times the ionization energy of the hydrogen atom. The Sobolev optical depth,  $\tau_S$ , for conditions during recombination is simply so large that the approximation of complete redistribution becomes unphysical.

Furthermore, at such large distances it is even questionable as to why one should be able to neglect variations of the black-body distribution, or the factor of  $1/\tilde{\nu}$  in the definition of  $\tau_{\text{abs}}$ . However, such an approximation is necessary to obtain the expression for the Sobolev escape probability. Obviously other corrections (e.g. related to two-photon processes, or the imbalance in the emission and absorption coefficient as mentioned in Sect. 2.2.4) will become important and *even necessary* to correct for these physical discrepancies. However, as we will see below, in spite of all these problems the Sobolev approximation at the level of  $\sim 10\%$  provides the correct answer for the escape probability, a fact that is very surprising.

### 3.2.2. Mean occupation number in the Lyman $\alpha$ and the Sobolev escape probability

To obtain the mean photon occupation number in the Lyman  $\alpha$  line we multiply (33) by  $\varphi$  and integrate over  $\nu$ . This then yields

$$\Delta \bar{n} = \bar{n} - \bar{n}^{\text{pl}} \approx \{p_{\text{em}} \bar{n} + p_d n_{\text{em}} - n_{\nu_{21}}^{\text{pl}}\} [1 - P_S] \quad (35a)$$

$$P_S = 1 - \int_0^1 d\chi e^{-\tau_S [1-\chi]} = \frac{1 - e^{-\tau_S}}{\tau_S} \stackrel{\tau_S \gg 1}{\approx} \frac{1}{\tau_S}, \quad (35b)$$

where we again have neglected the variation of  $n^{\text{pl}}$  over the line profile. Here  $P_S$  denotes the standard Sobolev escape probability (see Fig. 1 for its redshift dependence). After some rearrangement and with  $n_{\nu_{21}}^{\text{pl}} \approx \bar{n}^{\text{pl}}$ , Eq. (35a) can be cast into the final form

$$\bar{n}_{\text{cr}} = \bar{n}^{\text{pl}} + \frac{p_d(1 - P_S)}{p_d + p_{\text{sc}} P_S} [n_{\text{em}} - \bar{n}^{\text{pl}}] \quad (36a)$$

$$\equiv n_{\text{em}} - \frac{P_S}{p_d + p_{\text{sc}} P_S} [n_{\text{em}} - \bar{n}^{\text{pl}}] \quad (36b)$$

$$\stackrel{p_d \gg p_{\text{sc}} P_S}{\approx} n_{\text{em}} - \frac{P_S}{p_d} [n_{\text{em}} - \bar{n}^{\text{pl}}]. \quad (36c)$$

A solution similar to Eq. (36) was also given and discussed in Hummer & Rybicki (1992).

### 3.2.3. Relation to the expression which is normally used in multi-level recombination codes

But how does Eq. (36) actually relate to the expression

$$\bar{n}_{\text{st}} \approx n_L - P_S [n_L - \bar{n}^{\text{pl}}] \equiv \bar{n}^{\text{pl}} + [n_L - \bar{n}^{\text{pl}}](1 - P_S) \quad (37)$$

that is normally used (cf. Seager et al. 2000) in computations of the hydrogen recombination problem? To understand this connection the key ingredient is the quasi-stationary solution for the 2p population. In fact this approximation should *always* be possible, even if the spectral evolution is non-stationary, simply because the re-adjustment of the 2p population after some changes in the spectrum is so fast.

With Eqs. (10) and (30), the rate equation governing the time evolution of the 2p state can be cast in the form

$$N_{\text{H}} \frac{dX_{2\text{p}}}{dt} = R_{2\text{p}}^+ - N_{2\text{p}} R_{2\text{p}}^- + A_{21} N_{2\text{p}} \left[ \frac{\bar{n}}{n_{\text{L}}} - 1 \right], \quad (38)$$

where we directly neglected induced terms, and introduced  $X_{2\text{p}} = N_{2\text{p}}/N_{\text{H}}$ , where  $N_{\text{H}}$  denotes the total number density of hydrogen nuclei. With  $\frac{dX_{2\text{p}}}{dt} \approx 0$  one readily finds

$$N_{2\text{p}}^{\text{qs}} \approx \frac{R_{2\text{p}}^+}{A_{21} + R_{2\text{p}}^- - A_{21} \frac{\bar{n}}{n_{\text{L}}}} = \frac{p_{\text{d}} n_{\text{L}}}{n_{\text{L}} - p_{\text{em}} \bar{n}} \frac{R_{2\text{p}}^+}{R_{2\text{p}}^-}. \quad (39)$$

Inserting this into Eq. (18b) therefore yields

$$n_{\text{L}} \approx p_{\text{em}} \bar{n} + p_{\text{d}} n_{\text{em}}. \quad (40)$$

If we now use this in Eq. (35) one immediately finds  $\bar{n}_{\text{cr}} \equiv \bar{n}_{\text{st}}$ . Therefore the result (36) is completely equivalent to Eq. (37).

However, in one case factors are expressed in terms of  $n_{\text{em}}$ , while in the other case  $n_{\text{L}}$  is used. From Eqs. (36b) and (37) with  $\bar{n}_{\text{cr}} \equiv \bar{n}_{\text{st}}$  one can easily show

$$n_{\text{em}} - \bar{n}^{\text{pl}} = \left( 1 + \frac{p_{\text{sc}} P_{\text{S}}}{p_{\text{d}}} \right) [n_{\text{L}} - \bar{n}^{\text{pl}}]. \quad (41)$$

This implies that  $n_{\text{em}} \approx n_{\text{L}}$ . However, since in the Lyman  $\alpha$  rate, Eq. (30), the main term ( $\sim n_{\text{L}}$ ) cancels, the small difference  $n_{\text{em}} - n_{\text{L}} = \frac{p_{\text{sc}} P_{\text{S}}}{p_{\text{d}}} [n_{\text{L}} - \bar{n}^{\text{pl}}]$  cannot be neglected. Replacing the first  $n_{\text{em}}$  in Eq. (36c) with this expression and neglecting terms  $O(P_{\text{S}}/p_{\text{d}})^2$  one can directly recover Eq. (37). However, here it is important that in Eq. (36c) there is partial cancellation of terms  $O(P_{\text{S}}/p_{\text{d}})$  from the first and second  $n_{\text{em}}$ , leaving a much smaller residual  $\sim P_{\text{S}} [n_{\text{L}} - \bar{n}^{\text{pl}}]$ .

### 3.3. Escape probability for the case of coherent scattering

In the absence of line scattering, or equivalently for *coherent scattering* in the lab frame, the solution of the transfer equation is given by Eq. (23). Under quasi-stationary conditions (and with  $\tilde{N}_x^{\text{pl}} \approx \tilde{N}_{x_{21}}^{\text{pl}}$ ) one again has  $\Theta^{\text{coh}}(z') = 1$ , and also it is possible to use  $\tau_{\text{abs}}^{\text{qs}} \approx p_{\text{d}} \tau_{\text{cr}}^{\text{qs}}$ , where  $\tau_{\text{cr}}^{\text{qs}}$  is defined by Eq. (31). Then one can write

$$\Delta N_{\nu}^{\text{coh,qs}}(z) = [N_{\text{em}} - N_{\nu_{21}}^{\text{pl}}] [1 - e^{-\tau_{\text{d}}} e^{\tau_{\text{d}} \chi}], \quad (42)$$

with  $\tau_{\text{d}} = p_{\text{d}} \tau_{\text{S}}$ .

#### 3.3.1. Spectral characteristics of the solution

Looking at Fig. 2 it is clear that  $\tau_{\text{d}} \ll \tau_{\text{S}}$  at all relevant redshifts, so that  $\Delta N_{\nu}^{\text{coh,qs}}(z)$  should change strongly much closer to the line center than in the complete redistribution case, Eq. (33). If we again want to estimate where the photon distribution (42) varies most rapidly, assuming that this happens in the blue wing of the Lyman  $\alpha$  line, we can find

$$x_{\text{D}} \approx \frac{a}{\pi} \frac{p_{\text{d}} \tau_{\text{S}}}{\ln 2}. \quad (43)$$

At  $z \sim 1100$  one has  $p_{\text{d}} \sim 10^{-4}$ , such that with Eq. (34) one has  $x_{\text{D}} \sim 30$  (see Fig. 3). This result is much closer to the solution that would be obtained when using the more realistic type-II redistribution for the Lyman  $\alpha$  resonance scattering process, where in the quasi-stationary approximation the photon distribution for typical conditions in our Universe strongly varies at distances of a few hundred Doppler width (e.g. see Rybicki & dell'Antonio 1994). We already checked this point and found very similar results (Chluba & Sunyaev 2009b).

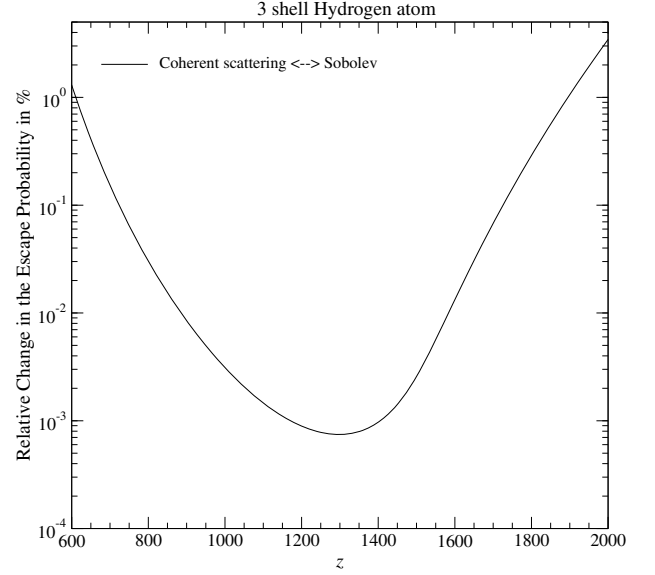


**Fig. 4.** Relative difference between the escape probability  $P_{\text{d}}^{\text{L}} = \frac{p_{\text{d}} P_{\text{d}}}{1 - p_{\text{em}} P_{\text{d}}}$  and the standard Sobolev escape probability,  $P_{\text{S}}$ . The death probability for a 3 shell hydrogen atom was used.

#### 3.3.2. Mean occupation number in the Lyman $\alpha$ and the escape probability

With (42) and the same simplifications that were mentioned above in connection with Eq. (36) one then obtains

$$\bar{n}_{\text{coh}} = n_{\text{em}} - P_{\text{d}} [n_{\text{em}} - \bar{n}^{\text{pl}}] \quad (44a)$$

$$P_{\text{d}} = \frac{1 - e^{-\tau_{\text{d}}}}{\tau_{\text{d}}} \stackrel{\tau_{\text{d}} \gg 1}{\approx} \frac{1}{p_{\text{d}} \tau_{\text{S}}} \approx \frac{P_{\text{S}}}{p_{\text{d}}}. \quad (44b)$$

Note that  $P_{\text{d}}$  is very similar to the standard Sobolev escape probability,  $P_{\text{S}} = [1 - e^{-\tau_{\text{S}}}] / \tau_{\text{S}}$ , with the only difference that in general  $\tau_{\text{d}} \leq \tau_{\text{S}}$  and hence  $P_{\text{d}} \geq P_{\text{S}}$  (cf. Figs. 1 and 2). Also one can directly see that in lowest order Eq. (44) is identical to Eq. (36c). This already suggests that in both the complete redistribution and the no line scattering approximation the answer for  $\bar{n}$  is nearly the same, with differences of the order  $O(P_{\text{S}}/p_{\text{d}})^2$ .

Again using the quasi-stationary solution for the 2p population, we can replace  $n_{\text{em}}$  applying the expression Eq. (40). Then solving for  $\bar{n}$  one finds

$$\bar{n}_{\text{coh}} \approx n_{\text{L}} - \frac{p_{\text{d}} P_{\text{d}}}{1 - p_{\text{em}} P_{\text{d}}} [n_{\text{L}} - \bar{n}^{\text{pl}}]. \quad (45)$$

Comparing this with the standard form Eq. (37), it is again clear that for  $p_{\text{em}} P_{\text{d}} \ll 1$  and  $\tau_{\text{S}} \gg \tau_{\text{d}} \gg 1$  one has  $\bar{n}_{\text{coh}} \approx \bar{n}_{\text{st}}$ . Looking at Fig. 1 shows that this should be the case at most of the redshifts relevant for the recombination of hydrogen, and that the differences between the complete redistribution and no scattering case should not exceed the level of  $\sim 10^{-3}$  in the redshift range  $800 \lesssim z \lesssim 1600$ .

In Fig. 4 we present a more detailed comparison and indeed find practically no important difference to the standard Sobolev case. This result is somehow surprising, since the assumption of complete redistribution leads to a totally different (and physically unrealistic) solution for the photon distribution. Still, the final result is comparable. This is due to the fact that the changes in the shape of the photon distribution are compensated by changes in the amplitude of the spectrum close to the line center, as already explained in connection with Eq. (41).



Note that in the case of 2 shells the differences would be much greater, since one can find  $P_d \sim 1$  at redshifts relevant for recombination (see Fig. 1). This again shows that one has to include at least 3 shells in the computation, in order to obtain meaningful results.

### 3.3.3. Escape probability in the limit $p_d \rightarrow 1$

It is also illustrative to look at the solution in the limit  $p_d \rightarrow 1$ . Physically, in the current formulation of the problem this should give the same answer as in the approximation of complete redistribution. This is because for  $p_d = 1$  every electron entering the 2p level via the Lyman  $\alpha$  channel will pass through the continuum or some higher shell, where it will forget its history. It will be replaced by another fresh electron, with a natural line profile, as in the complete redistribution approximation for a line scattering event.

From Eq. (45), with  $p_d = 1$ ,  $p_{sc} = 0$  and  $P_d \equiv P_S$ , it is quite obvious that  $\bar{n}_{\text{coh}} \equiv \bar{n}_{\text{cr}}$ , but can one also see this directly from Eq. (44a), which in the first place only leads to  $\bar{n}_{\text{coh}} = n_{\text{em}} - P_S[n_{\text{em}} - \bar{n}^{\text{pl}}]$ . Here apparently  $n_{\text{em}} \equiv n_L$ , a result that indeed can be confirmed with Eq. (40), so that also  $\bar{n}_{\text{coh}} \equiv \bar{n}_{\text{cr}}$  follows.

### 3.3.4. Until what distance from the line center is the shape of the photon distribution important?

The escape probability,  $P_d$ , was obtained from the integral over the Lyman  $\alpha$  line profile. If we only integrate up to some frequency  $\nu_m$ , then one has

$$P_d(\nu_m) = \int_0^{\nu_m} \varphi(\nu) e^{-\tau_d} e^{\tau_d \chi(\nu)} d\nu = \frac{e^{-\tau_d[1-\chi_m]} - e^{-\tau_d}}{\tau_d} \approx \frac{e^{-\tau_d[1-\chi_m]}}{\tau_d}, \quad (46)$$

with  $\chi_m = \chi(\nu_m)$ . Therefore the relative difference in the value of  $P_d$  is given by

$$\frac{\Delta P_d(\nu_m)}{P_d} = \frac{P_d(\nu_m) - P_d}{P_d} \approx e^{-\tau_d[1-\chi_m]} - 1 \underset{\tau_d[1-\chi_m] \ll 1}{\approx} -\tau_d[1-\chi_m]. \quad (47)$$

If we assume that  $\nu_m > \nu_{21}$  is already in the damping wing then with the approximation Eq. (A.2) of the Voigt profile one obtains

$$\frac{\Delta P_d(\nu_m)}{P_d} \approx -\frac{a}{\pi} \frac{\tau_d}{x_D}. \quad (48)$$

At  $z = 1100$  this yields  $\frac{\Delta P_d(\nu_m)}{P_d} = -16\% \left[ \frac{x_D}{100} \right]^{-1}$ , so that in the no-scattering approximation for  $\sim 10\%$ ,  $\sim 1\%$ , and  $\sim 0.1\%$  accuracy one has to know the spectrum up to  $x_D \sim 10^2$ ,  $x_D \sim 10^3$ , and  $x_D \sim 10^4$ . This shows how important the knowledge of the solution for the photon distribution in the distant wings is.

In the case of complete redistribution one can easily show that  $\frac{\Delta P_S(\nu_m)}{P_S} = -16\% \left[ \frac{x_D}{10^6} \right]^{-1}$  at  $z = 1100$ . This implies that for  $\sim 10\%$ ,  $\sim 1\%$ , and  $\sim 0.1\%$  accuracy one has to know the spectrum up to  $x_D \sim 10^6$ ,  $x_D \sim 10^7$ , and  $x_D \sim 10^8$ . Let us emphasize again that these are extremely large (even unphysical) distances from the Lyman  $\alpha$  resonance. However, it is in these regions where the value of the Sobolev escape probability is formed.

### 3.4. Effective escape probability using the time-dependent solution

With the solution (23) we can also describe the time-dependence of  $\bar{n}$  within the approximation of coherent scattering in the lab

frame. Although one does expect some modifications when accounting for partial frequency redistribution, our computations (Chluba & Sunyaev 2009b) show that the additional correction will be dominated by the influence of line recoil<sup>10</sup>, which has been addressed in Grachev & Dubrovich (2008). However, the time-dependent correction that is considered here turns out to be much larger, so that we shall focus on this only. Below we now provide a detailed discussion of the time-dependent correction in the case of coherent scattering in the lab frame, introducing an effective escape probability, which then can be used in computations of the cosmological recombination history.

#### 3.4.1. Escape probability during recombination without redistribution but with full time-dependence

Using the time-dependent solution for the case of no redistribution, Eq. (23), it is possible to write

$$\begin{aligned} \bar{n}^{\text{coh}}(z) &= \bar{n}^{\text{pl}} + \frac{c^2}{2\nu_{21}^2} \int_0^\infty \varphi(\nu) \Delta N_\nu^{\text{coh}}(z) d\nu \\ &= \bar{n}^{\text{pl}} + \Delta \bar{n}_{\text{em}}(z) \int_0^\infty \varphi(\nu) d\nu \int_{z_s}^z \Theta^{\text{coh}}(z') \partial_{z'} e^{-\tau_{\text{abs}}(\nu, z', z)} dz' \\ &= \bar{n}^{\text{pl}} + \Delta \bar{n}_{\text{em}}(z) (1 - P_{\text{em}}^t) \end{aligned} \quad (49a)$$

$$P_{\text{em}}^t = 1 + \int_0^\infty \varphi(\nu) d\nu \int_z^{z_s} \Theta^{\text{coh}}(z') \partial_{z'} e^{-\tau_{\text{abs}}(\nu, z', z)} dz', \quad (49b)$$

where we have  $\Delta \bar{n}_{\text{em}}(z) = n_{\text{em}} - \bar{n}^{\text{pl}}$ .

Here it is very important to mention that one has to use  $\Theta^{\text{coh}}(z)$  as defined by Eq. (23b) but evaluate the blackbody distribution at the line center *only*, i.e. use  $\Theta^{\text{coh}}(z') \approx [\tilde{N}_{\text{em}}(z') - \tilde{N}_{x_{21}^{\text{pl}}}] / [\tilde{N}_{\text{em}}(z) - \tilde{N}_{x_{21}^{\text{pl}}}]$  with  $x_{21}^{\text{pl}} = \nu_{21}/[1+z']$ . This is necessary in order to be consistent with the formulation of line emission and absorption processes, which, as mentioned in Sect. 2.2.4, in full equilibrium does not exactly conserve a blackbody distribution. A more consistent formulation will be given in a future paper, but the result for the pure time-dependent correction should be very similar.

Equation (49a) provides the time-dependent solution for  $\bar{n}(z)$ , when the ionization history is known until  $z$ . However, in real calculations Eq. (49a) is not very useful, since the evaluation of the integral is rather time-consuming. With Eq. (49b) we defined an *effective escape probability*, which can be compared with the result in the full quasi-stationary case. The differences will be due to non-stationary contributions in the evolution of the photon distribution, and can be iteratively used in computations of the recombination history. Since the correction is expected to be small, even the first iteration should give a rather good answer.

To obtain the difference from the Sobolev escape probability, one again has to use the quasi-stationary solution for the 2p state, leading to relation (40). With this one can eliminate  $n_{\text{em}}$  from 49, and bring the expression for  $\bar{n}$  in the standard form (37). This yields

$$\bar{n}^{\text{coh}}(z) = n_L - P_{\text{esc}}^L [n_L - \bar{n}^{\text{pl}}] \quad (50a)$$

$$P_{\text{esc}}^L = \frac{p_d P_{\text{em}}^t}{1 - p_{\text{sc}} P_{\text{em}}^t}. \quad (50b)$$

<sup>10</sup> Including atomic recoil we find a correction of  $\Delta P/P \sim 4\%$  at  $z \sim 1100$  and  $\Delta P/P \sim 6\%$  at  $z \sim 800$  to the Sobolev escape probability, which, in reasonable agreement with Grachev & Dubrovich (2008), leads to  $\Delta N_e/N_e \sim -1.2\%$  at  $z \sim 950$ .

Now  $P_{\text{esc}}^{\text{L}}$  can be directly compared with the Sobolev escape probability.

Looking at (49b) it is clear that there are two sources for the time-dependent correction. The first comes from the time-dependence of  $\Theta^{\text{coh}}$ , while the second is due to modifications in the absorption optical depth,  $\tau_{\text{abs}}$ . Below we now discuss each correction separately.

### 3.4.2. Neglecting the time-dependence of $\Theta^{\text{coh}}$

If we set  $\Theta^{\text{coh}} = 1$  in Eq. (49b) one obtains

$$P_{\text{em}}^{\text{t},0}(z) = \int_0^\infty \varphi(\nu) e^{-\tau_{\text{abs}}(\nu, z_s, z)} d\nu. \quad (51)$$

With this expression it is possible to take into account the time-dependent corrections that are only due to the modifications of  $\tau_{\text{abs}}$  in comparison to the quasi-stationary case (see Sect. 3.3).

First, it is clear that due to the  $\nu$ -dependence of the absorption cross section the total absorption optical depth depends strongly on the initial frequency of the emitted photon. For example, if a photon is emitted on the blue side of the Lyman  $\alpha$  resonance, then after some redshifting it will come close to the Doppler core of the Lyman  $\alpha$  line, where it will be absorbed with extremely high probability. Depending on the initial distance to the Doppler core, this will take some time, during which the properties of the medium (e.g. the ionization degree) may have changed significantly. Similarly, photons emitted in the very distant red wing of the Lyman  $\alpha$  line may redshift for a very long time, before they will be reabsorbed, if at all.

At high  $z$  the total absorption optical depth is expected to mainly vary due to the changes in the number density of ionized hydrogen atoms, and at low redshifts because of the steep drop in  $p_{\text{d}}$ . If for given initial frequency  $\nu'$  of an emitted photon the time it takes until this photon is reabsorbed ( $\tau_{\text{abs}} \sim 1$ ) is similar to the Hubble time, then these changes may be important.

If the considered photon was emitted close to the Lyman  $\alpha$  line center, the absorption optical depth is dominated by its value inside the Doppler core, where photons only travel a very short distance (a small fraction of the Doppler width), before being reabsorbed. In this case, the quasi-stationary approximation certainly is valid with very high accuracy, since  $\Delta\nu/\nu \ll 1$  between emission and absorption implies  $\Delta z/z \ll 1$ , so that the medium has not changed very much. However, when the photon is initially released in the distant red or blue wing of the Lyman  $\alpha$  resonance, it can redshift for a much longer time before being reabsorbed, so that changes in the medium, in particular the ionization degree and death probability, may play an important role.

In Fig. 5 we show the direct comparison of the escape probability that follows from Eq. (51) with the Sobolev escape probability. At very low and very high redshifts the correction due to the pure time-dependence of  $\tau_{\text{abs}}$  becomes very small. The difference that is seen close to  $z \sim 600$  and  $z \sim 1800$  is only related to the correction coming from the coherent scattering approximation (see Fig. 4). In both cases this behavior can be explained by the fact that the importance of the wings for the total value of the escape probability decreases. Photons escape directly from the Doppler core, so that the contributions to the value of  $P_{\text{em}}^{\text{t},0}(z)$  can be considered quasi-stationary.

To understand the behavior at intermediate redshift, it is important that before the maximum of  $\tau_{\text{d}}$  around  $z_{\text{max}} \sim 1300$  (cf. Fig. 2), one expects that independent<sup>11</sup> of the considered

<sup>11</sup> This statement is not completely correct, since in Eq. (22b) we do take into account the factor  $1/\nu$ . However, this only affects the very distant blue wing.

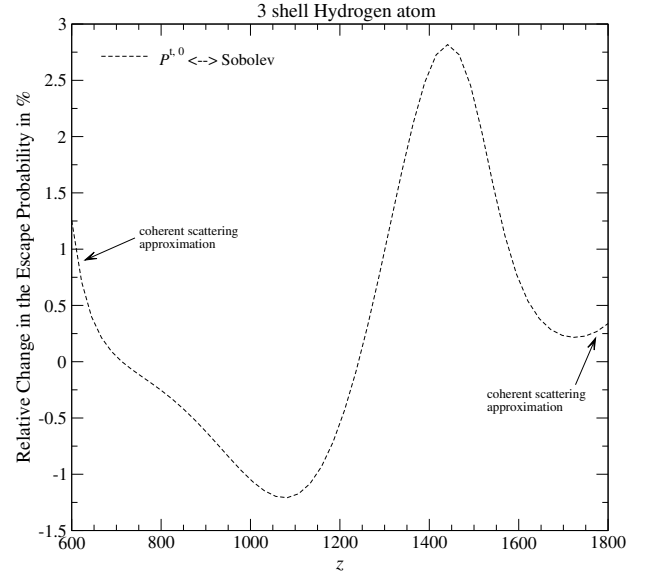


Fig. 5. Differences between the escape probability  $P = \frac{p_{\text{d}} P_{\text{em}}^{\text{t},0}}{1 - p_{\text{sc}} P_{\text{em}}^{\text{t},0}}$ , where  $P_{\text{em}}^{\text{t},0}(z)$  is given by Eq. (51), and the standard Sobolev escape probability,  $P_{\text{S}}$ . We used the death probability for the 3 shell hydrogen atom.

frequency,  $\tau_{\text{abs}}(\nu, z', z)$  is smaller than in the quasi-stationary approximation  $\tau_{\text{abs}}^{\text{qs}}(\nu, z', z) = \tau_{\text{d}}(z) \int_{\nu'}^{\nu} \varphi(\nu'') d\nu''$ . This is simply because at  $z' > z \gtrsim z_{\text{max}}$  the value of  $\tau_{\text{d}}(z') \lesssim \tau_{\text{d}}(z)$ . At those times the time-dependent modifications of  $\tau_{\text{abs}}$  should therefore result in a positive correction to the effective escape probability (cf. Fig. 5). With a similar argument, at redshift  $z \lesssim 1300$  the correction in the escape probability should be negative, as is seen in Fig. 5.

### 3.4.3. Correction due to the time-dependence of $\Theta^{\text{coh}}$

In Sect. 3.4.2 we have neglected the time-dependence of  $\Theta^{\text{coh}}$ . This factor describes how much the photon emission process varies as a function of time, which in the present approximation is independent of frequency (see comment in Sect. 3.4.1).

With Eqs. (51) and (49b) one can define

$$\begin{aligned} \Delta P_{\text{em}}^{\text{t}} &= \int_0^\infty \varphi(\nu) d\nu \int_z^{z_s} [\Theta^{\text{coh}}(z') - 1] \partial_{z'} e^{-\tau_{\text{abs}}(\nu, z', z)} dz' \\ &= - \int_0^\infty \varphi(\nu) \Delta F(\nu) d\nu \end{aligned} \quad (52a)$$

$$\Delta F(\nu) = \int_{z_s}^z [\Theta^{\text{coh}}(z') - 1] \partial_{z'} e^{-\tau_{\text{abs}}(\nu, z', z)} dz'. \quad (52b)$$

With this expression it is now possible to calculate<sup>12</sup> the additional correction to the escape probability coming from the variation of  $\Theta^{\text{coh}}$  over time.

In order to understand the final result we first consider the behavior of the inner integrand (52a) at different stages of hydrogen recombination. Since the function  $F(\nu) = \int_{z_s}^z \Theta^{\text{coh}}(z') \partial_{z'} e^{-\tau_{\text{abs}}(\nu, z', z)} dz'$  is identical to the Lyman  $\alpha$  spectral distortion in the no redistribution approximation, but normalized

<sup>12</sup> The evaluation of the integral (52a) is rather cumbersome. It is most important that for a fixed frequency  $\nu$  at redshift  $z$  the inner integral varies most strongly at  $z' \sim \max(z, \nu_{21}(1+z)/\nu)$ .

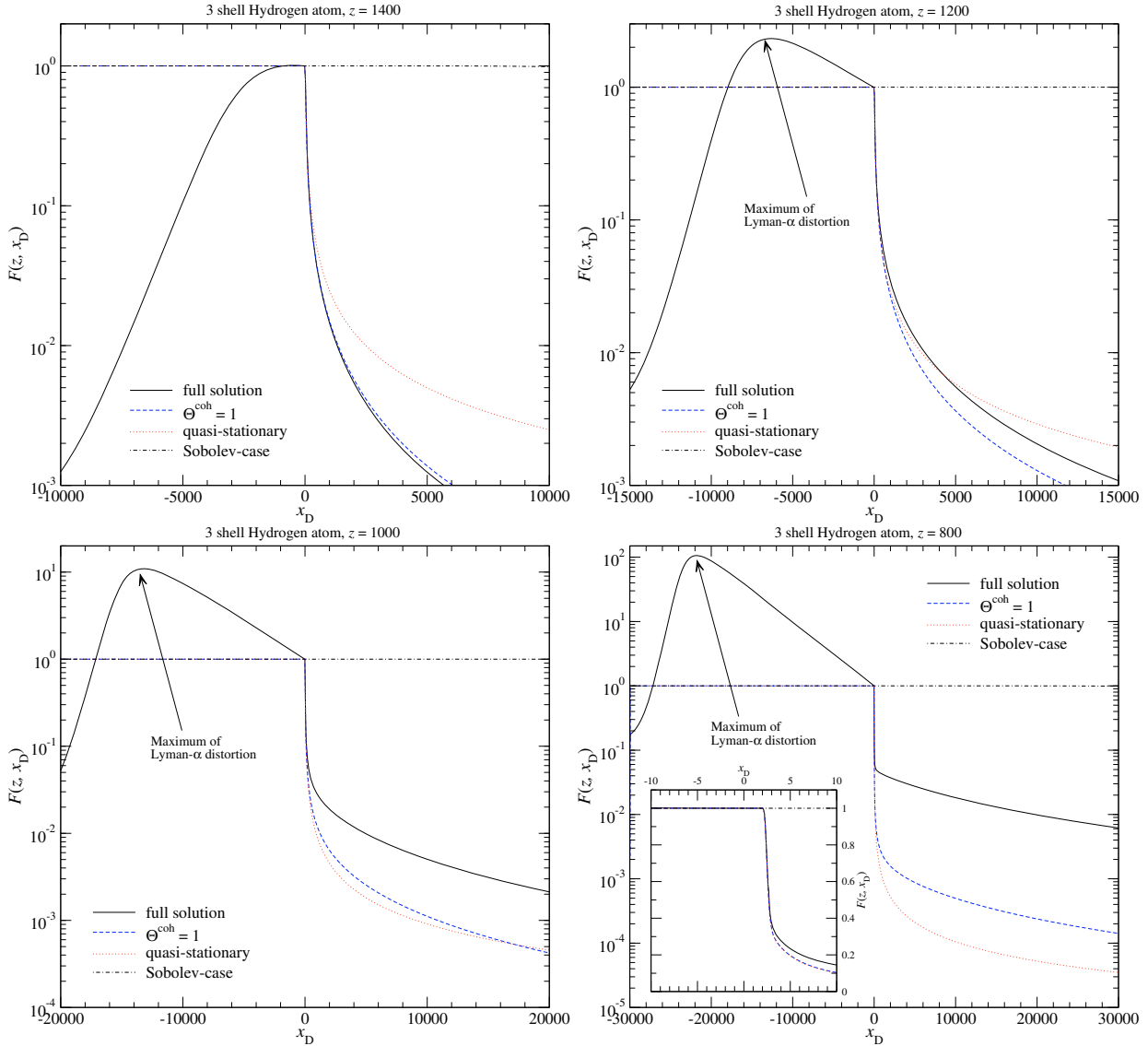


**Fig. 6.** The spectral distortion  $\Delta N_\nu$  far away from the Lyman  $\alpha$  line center at different stages of hydrogen recombination. In all cases redistribution of photons over frequency was neglected. We normalized the distortion to unity at the Lyman  $\alpha$  frequency, i.e.  $F \equiv \Delta N_\nu(z)/\Delta N_{\nu_{21}}(z)$ . The dotted curves give the spectral distortion in the quasi-stationary approximation,  $F^{\text{qs}}(\nu) = 1 - e^{-\tau_d} e^{\tau_d \chi(\nu)}$ . For the dashed curves we neglected the variation of  $\Theta^{\text{coh}}$  in the solution (23), leading to  $F_0(\nu) = 1 - e^{-\tau_{\text{abs}}(\nu; z_s, z)}$ , with  $z_s \rightarrow \infty$ . The solid lines show the spectral distortion in the time-dependent case, i.e.  $F(\nu) = F_0(\nu) + \Delta F(\nu)$ , where  $\Delta F(\nu)$  is defined by Eq. (52b). For comparison, the dash-dotted curves give the spectral distortion in the Sobolev approximation,  $F^{\text{S}}(\nu) = 1 - e^{-\tau_{\text{S}}} e^{\tau_{\text{S}} \chi(\nu)}$ . We also indicated the position of the maximum of the redshifted Lyman  $\alpha$  distortion, which appeared at redshift  $z \sim 1400$ .

to its value at the line center, i.e.  $F(\nu) \equiv \Delta N_\nu(z)/\Delta N_{\nu_{21}}(z)$ , it is illustrative to define

$$F^{\text{qs}}(\nu) = 1 - e^{-\tau_d} e^{\tau_d \chi(\nu)} \quad (53a)$$

$$F_0(\nu) = 1 - e^{-\tau_{\text{abs}}(\nu; z_s, z)} \quad (53b)$$

$$F(\nu) = F_0(\nu) + \Delta F(\nu), \quad (53c)$$

in addition to Eq. (52b). Here  $F^{\text{qs}}(\nu)$  represents the Lyman  $\alpha$  spectral distortion in the full quasi-stationary approximation, for  $F_0(\nu)$  only the variation of  $\Theta^{\text{coh}}$  is neglected, and  $F(\nu)$  is the time-dependent distortion in the no redistribution approximation. From these functions the corresponding escape probabilities can be obtained by  $P_{\text{esc}} = 1 - \int \varphi(\nu) F(\nu) d\nu$ , which then can be inserted in Eq. (50b) when comparing with  $P_{\text{S}}$ . Therefore it is clear that if  $F(\nu) < F^{\text{qs}}(\nu)$  at all frequencies, the resulting effective escape probability should be slightly larger than  $P_d$ .

In Figs. 6 and 7 we illustrate the behavior of the functions (53) at different stages of hydrogen recombination. We

used the solution for the populations in the 3 shell case as given by our multi-level code (Rubiño-Martín et al. 2006; Chluba et al. 2007). As expected, in all cases  $F^{\text{qs}}(\nu)$  and  $F_0(\nu)$  are very close to unity at  $x_D \lesssim 0$  and then drops very fast toward zero at  $x_D \gtrsim 0$ . Also Fig. 7 clearly shows that  $F^{\text{qs}}(\nu) \approx F_0(\nu)$  in the red wing and the Doppler core of the Lyman  $\alpha$  resonance. This is expected, since at  $\nu \lesssim \nu_{21}$  always  $\tau_{\text{abs}} \gg 1$ , so that its exact value does not matter. Furthermore we can observe a change in the sign of the difference  $F_0(\nu) - F^{\text{qs}}(\nu)$  in the blue wing when going from high to lower redshift. At  $z = 1400$  one can clearly see that  $F_0(\nu) < F^{\text{qs}}(\nu)$  in the range  $0 \lesssim x_D \lesssim 100$ , so that  $P_{\text{em}}^{l,0}(z) > P_d$  is expected, in agreement with the results presented in Fig. 5. On the other hand, in all the other cases shown  $F_0(\nu) > F^{\text{qs}}(\nu)$  at  $0 \lesssim x_D \lesssim 100$  so that one should find  $P_{\text{em}}^{l,0}(z) < P_d$ , again confirming the results given in Fig. 5.

Because of the steep drop of  $F^{\text{qs}}(\nu)$  and  $F_0(\nu)$  at a few Doppler width above the line center, the main contribution to

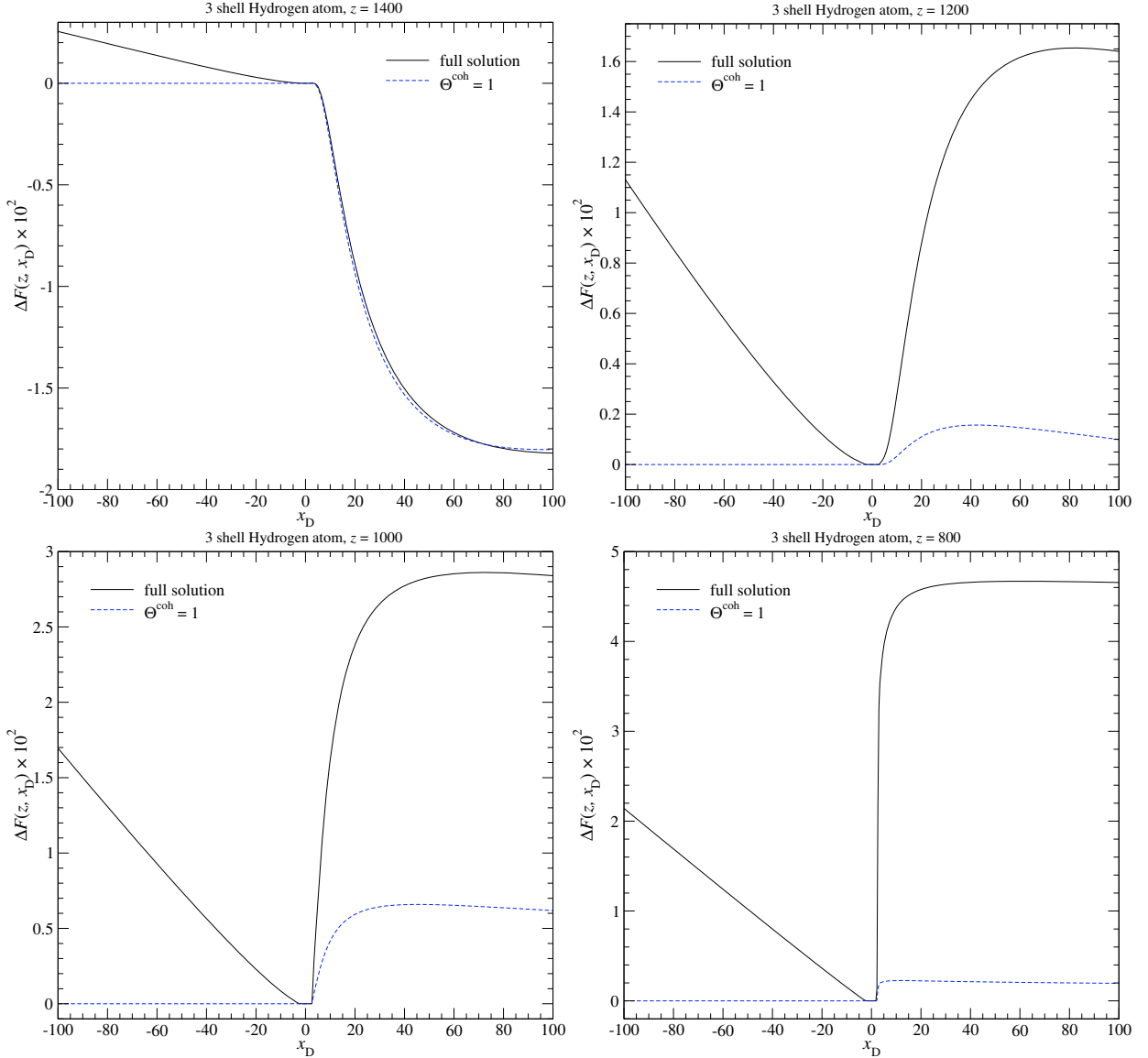


**Fig. 7.** The spectral distortion  $\Delta N_\nu$  close to the Lyman  $\alpha$  line center at different stages of hydrogen recombination. In all cases redistribution of photons over frequency was neglected. We normalized the distortion to unity at the Lyman  $\alpha$  frequency, i.e.  $F \equiv \Delta N_\nu(z)/\Delta N_{\nu_{21}}(z)$  and show the difference to the quasi-stationary solution,  $F^{\text{qs}}(\nu) = 1 - e^{-\tau_d} e^{\tau_d \chi(\nu)}$ . For the dashed curves we neglected the variation of  $\Theta^{\text{coh}}$  in the computation of the escape probability, while for the solid lines the spectral distortion in the time-dependent case was taken into account.

the escape probability clearly comes from rather close to the line center. However, at the level of percent the shape of the distortion up to a few hundred or thousand Doppler widths is important.

If we now look at the spectral distortion in the time-dependent approximation,  $F(\nu) = F_0(\nu) + \Delta F(\nu)$ , we can see that at *all* stages the variations of  $\Theta^{\text{coh}}$  with redshift become important outside the Doppler core. From Fig. 6 we can distinguish in more detail the following regimes: (i) at redshifts  $z \gtrsim 1400$  the distant wing distortion is *smaller* than in the quasi-stationary approximation. This is because at redshifts much before the time under consideration the emission in the Lyman  $\alpha$  transition was very inefficient, so that until then not many photons can have appeared or reached large distances from the Lyman  $\alpha$  line. The slope of the red wing distortion is positive close to the line center; (ii) at redshifts  $z \lesssim 1400$  the distortion in the blue wing and nearby red wing is *greater* than in the quasi-stationary approximation. The production rate of Lyman  $\alpha$  photons has already passed its maximum (at  $z \sim 1400$ ), so that at the current line

center *fewer* photons are produced the lower the redshift becomes. The slope of the red wing distortion is negative close to the line center.

It is also clear that in case (i) the value of  $\Delta \bar{n}$  is *smaller* than in the quasi-stationary approximation, while it is expected to be *larger* in case (ii). According to the definition 49 this implies that in the former case the effective escape probability is *higher* than in the quasi-stationary approximation, while it is *lower* in the latter case. In Fig. 8 we can see that these expectations are true (see solid line). The total correction due to excess or a deficit of photons leads to a total decrease of the effective escape probability at  $z \lesssim 1400$  that reaches  $\Delta P/P \sim -5.8\%$  at  $z \sim 1140$ , while it results in an increase of  $\Delta P/P \sim +3.7\%$  at  $z \sim 1510$ .

Although in the escape integral the distortion in the vicinity of the line center mainly contributes, at the percent level the distant wings are also important. As we have seen in Fig. 6 the red wing distortion due to the Lyman  $\alpha$  transition can exceed the distortion close to the line center by a large amount. In this

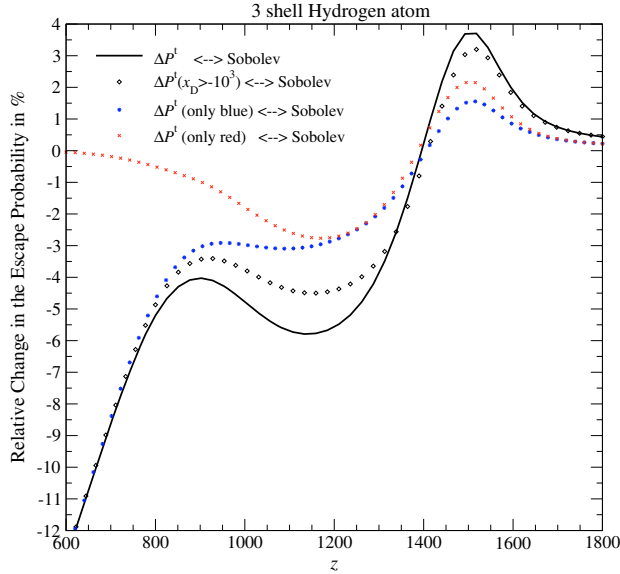


**Fig. 8.** Correction to the Sobolev escape probability due to variations of  $\Theta^{\text{coh}}$ . For the solid curve we used  $\Delta P_{\text{em}}^l(z)$  according to Eq. (52). The boxed curve was computed with Eq. (52), but including the variation of  $\Theta^{\text{coh}}$  only at  $x_D \geq -10^3$ . The other two curves were obtained setting  $\Theta^{\text{coh}} = 1$  in the red wing (stars) or blue wing (crosses), respectively.

case the question is how much the very distant wings actually contribute to the total correction shown in Fig. 8. For this we computed  $\Delta P_{\text{em}}^l(z)$ , but excluding the correction at  $x_D \leq -10^3$ . Looking at the boxed curve in Fig. 8 shows that the very distant red wings contribute about  $\Delta P/P \sim 0.6\%$  at  $z \sim 1500$ , and  $\Delta P/P \sim -1.3\%$  at  $z \sim 1100$ . This is an important point, since in the very distant wings other processes related to the formulation of the problem will also become important (i.e. due to changes in the absorption profiles, when considering the problem as a two-photon process), so that one expects additional revisions for contributions from the very distant wings. However, here the corrections mainly seem to come from regions in the vicinity ( $|x_D| \lesssim 10^2 - 10^3$ ) of the Lyman  $\alpha$  line center.

At low redshifts ( $z \lesssim 800 - 900$ ) one can observe an additional strong decrease in the effective escape probability. This is due to the additional re-excitation of electrons by the distortion on the blue side of the Lyman  $\alpha$  resonance. Most of the photons in this part of the spectrum have been emitted much earlier, at times around the maximum of the Lyman  $\alpha$  emission ( $z \sim 1400$ ). This also explains the huge difference to the quasi-stationary solution: as one can see in Fig. 6, at  $z \lesssim 800$  the amount of photons exceeds the spectral distortion obtained in the quasi-stationary approximation by about two orders of magnitude. The spectral distortion is only a factor of  $\sim 100$  below the emission in the line center. Looking at Fig. 7, very close to the Lyman  $\alpha$  line center some differences also are visible, which at the percent level do matter.

To show that the distortions on the blue side of the Lyman  $\alpha$  are responsible for this re-excitation we also computed the correction only including the non-stationary contributions for the red side, but setting  $\Theta^{\text{coh}} = 1$  for evaluations on the blue side. The result is also shown in Fig. 6 (stars). For completeness we also gave the curve when *only* including the corrections on the blue side of the line. As one can see, at  $z \gtrsim 1100$  the red and blue wing corrections are very similar. However, at low redshifts the blue wing correction clearly dominates, supporting the

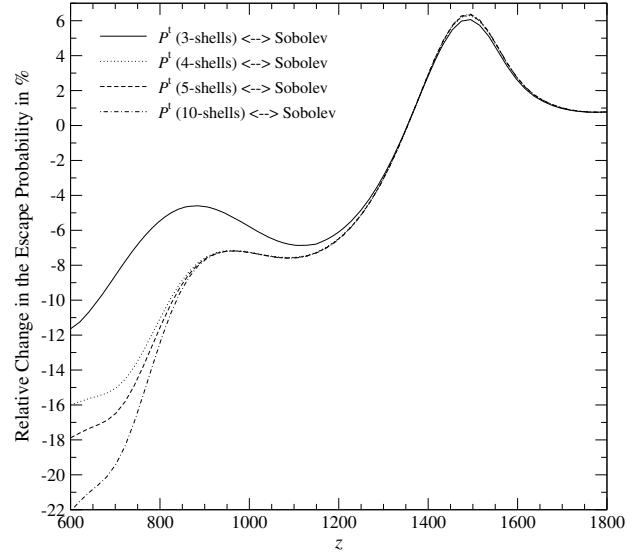


**Fig. 9.** Total correction to the Sobolev escape probability. All curves were computed using the time-dependent solution according to Eq. (49b), but including a different number of shells.

statement made above. Again one can expect some changes in the conclusions when treating the problem in the full two-photon formulation, since the emission of photons at high frequencies will be significantly less in the two-photon treatment, simply due to the fact that due to energy conservation the emission profiles do not extend to arbitrarily high frequencies (e.g. see Chluba & Sunyaev 2008). However, the corrections to the escape probability at  $z \lesssim 800$  do not propagate very strongly to the ionization history, so that here we do not consider this unphysical aspect of the solution any further.

#### 3.4.4. Dependence of the effective escape probability on the included number of hydrogen shells

Although the death probability  $p_d$  does not depend on the solution of the recombination problem, the amount of fresh electrons injected into the Lyman  $\alpha$  line depends on the populations of the excited states. Therefore the strength of the Lyman  $\alpha$  line strongly depends on the total number of shells that are included (Rubino-Martín et al. 2006). Here in particular the low-redshift tail ( $z \lesssim 800$ ) will be affected, and hence there one also expects changes in the correction to the effective escape probability.

In Fig. 8 we show the differences in the escape probability when including more shells. We used the numerical solution for the excited levels as obtained with our multi-level hydrogen code (Chluba et al. 2007). At redshifts  $z \gtrsim 1200$  the result is practically unaffected by the total number of hydrogen shells that are included. In particular the result seems converged when including  $\sim 4-5$  shells, leading to a total correction of  $\Delta P/P \sim -7.6\%$  at  $z \sim 1100$ , while it results in an increase of  $\Delta P/P \sim +6.4\%$  at  $z \sim 1490$ . At redshifts  $900 \lesssim z \lesssim 1200$ , some small changes are still visible when including more than 3 shells, but again the result seems to remain unchanged when including more than  $\sim 4-5$  shells. For the computation of the CMB power spectra the corrections in this range are most important (see Sect. 4).

At lower redshifts, however, the result still changes notably. At  $z \sim 600$  the correction increases by about 6.4% when including 5 shells, and for 10 shells even by about 10%. This can be explained when realizing that the total emission in the Lyman  $\alpha$  line at low redshifts becomes less when including more shells.

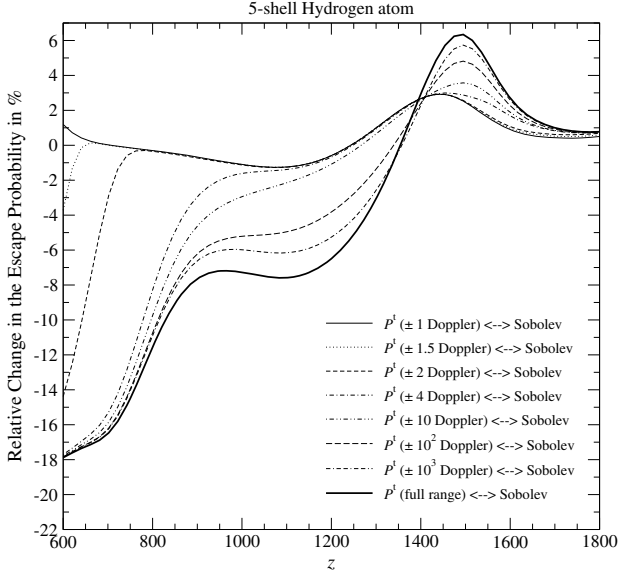


**Fig. 10.** Total correction to the Sobolev escape probability for the 5 shell hydrogen atom. All curves were computed using the time-dependent solution,  $P_{\text{em}}^{\text{t}} = P_{\text{em}}^{\text{t}0} + \Delta P_{\text{em}}^{\text{t}}$  according to Eqs. (49b), (51) and (52). The term  $P_{\text{em}}^{\text{t}0}$  was fully included, but for the contribution from  $\Delta P_{\text{em}}^{\text{t}}$  the time-dependent correction was only taken into account for a given central region  $|x_{\text{D}}| \leq \text{const}$  around the resonance, as labeled respectively.

Therefore the wing emission from redshifts around the maximum of the Lyman  $\alpha$  emission ( $z \sim 1400$ ), which practically remains unchanged, becomes more important, being able to re-excite the 2p state as explained in the previous paragraph. As we mentioned already this aspect will probably be affected when including corrections to the emission and absorption profiles according to the two-photon formulation. Furthermore, as we will see in the next Sect. this low redshift tail is not so important for the predictions of the CMB power spectra.

### 3.4.5. Dependence of the effective escape probability on the distance from the line center

As a last point, we want to answer the question of where in the case of  $\Delta P_{\text{em}}^{\text{t}}$  the main correction actually comes from. We have already seen in Sect. 3.4.3 that the very distant red wing contributes at the level of percent. Also we have seen that at redshifts  $z \gtrsim 800$ –900 the blue and red sides of the Lyman  $\alpha$  line give similar contributions, while at low redshift due to the self-feedback the blue wing clearly dominates.

In Fig. 10 we show the total correction to the Sobolev escape probability when only including the time-dependent correction for a given central region around the resonance in the computation of  $\Delta P_{\text{em}}^{\text{t}}$ . It is obvious that the innermost Doppler core ( $\pm 1$  Doppler width) does not contribute much to the result. This is expected, since there the photon distribution should evolve as in the quasi-stationary approximation, with very high accuracy. This fact can also be seen in Fig. 7, where close to the line center the deviation of the photon distribution for the quasi-stationary solution is very small.

At low redshifts ( $z \lesssim 800$ –900) the region up to  $\pm 4$  to  $\pm 10$  Doppler width seems to be quite important. As explained in Sect. 3.4.3, there the correction is mainly because of self-feedback, which is strongest where photons really are reabsorbed. However, at practically all other redshifts one can clearly see that the distant wings contribute significantly. Even within

$\pm 10^3$  Doppler width the deviations of the spectrum from the quasi-stationary solution are important.

### 3.5. Dependence of the escape probability on the shape of the emission and absorption profile

As mentioned in the introduction, in the Sobolev approximation it is well known that the result for the escape probability does not depend on the shape of the Lyman  $\alpha$  emission profile. Looking at the derivation of expression 35b for  $P_{\text{S}}$  it is clear that in addition to the condition of quasi-stationarity one needs  $\phi_{\text{em}} \equiv \phi_{\text{abs}} \equiv \phi_{\text{sc}}$ , i.e. the equality of the line emission, line absorption, and line scattering profile. This conclusion is also reached in the case of no line scattering (Sect. 3.3) leading to  $P_{\text{d}}$  as given by Eq. (44b).

However, if  $\phi_{\text{em}} \neq \phi_{\text{abs}}$  then the situation is more complicated. Starting with Eq. (20), but allowing  $\phi_{\text{em}} \neq \phi_{\text{abs}}$ , one can find the solution

$$\Delta N_{\nu}^{\text{a}}(z) = [N_{\text{em}}(z) - N_{\nu_{21}}^{\text{pl}}(z)] \int_{z_{\text{s}}}^{\infty} \Theta^{\text{a}}(z') \partial_{z'} e^{-\tau_{\text{abs}}(\nu, z', z)} dz', \quad (54a)$$

$$\Theta^{\text{a}}(z') = \frac{\tilde{N}_{\text{em}}(z') \times \frac{\phi_{\text{em}}(z', \nu_{z'})}{\phi_{\text{abs}}(z', \nu_{z'})} - \tilde{N}_{x}^{\text{pl}}}{\tilde{N}_{\text{em}}(z) - \tilde{N}_{x_{21}}^{\text{pl}}} \quad (54b)$$

with  $\nu_{z'} = \nu \frac{1+z'}{1+z}$ , and  $\tau_{\text{abs}}(\nu, z', z)$  as defined by Eq. (22) but replacing  $\phi \rightarrow \phi_{\text{abs}}$ . With this, the mean occupation number in the Lyman  $\alpha$  line can be directly computed leading to

$$\begin{aligned} \bar{n}^{\text{coh}}(z) &= \bar{n}^{\text{pl}} + \frac{c^2}{2\nu_{21}^2} \int_0^{\infty} \varphi_{\text{abs}}(\nu) \Delta N_{\nu}^{\text{a}}(z) d\nu \\ &= \bar{n}^{\text{pl}} + \Delta \bar{n}_{\text{em}}(z) \int_0^{\infty} \varphi_{\text{abs}}(\nu) d\nu \int_{z_{\text{s}}}^{\infty} \Theta^{\text{a}}(z') \partial_{z'} e^{-\tau_{\text{abs}}(\nu, z', z)} dz' \\ &= \bar{n}^{\text{pl}} + \Delta \bar{n}_{\text{em}}(z) (1 - P_{\text{em}}^{\text{a}}) \end{aligned} \quad (55a)$$

$$P_{\text{em}}^{\text{a}} = 1 + \int_0^{\infty} \varphi_{\text{abs}}(\nu) d\nu \int_z^{z_{\text{s}}} \Theta^{\text{a}}(z') \partial_{z'} e^{-\tau_{\text{abs}}(\nu, z', z)} dz', \quad (55b)$$

with the same definitions as in Eq. (49). Note that here one has to compute  $\bar{n}$  using the absorption profile function. Now it is easy to show that for  $\Theta^{\text{a}} = 1$ ,  $\tau_{\text{abs}} = p_{\text{d}} \tau_{\text{S}} \chi$ , and  $\phi_{\text{em}} \equiv \phi_{\text{abs}} = \phi$ , one directly obtains the solution Eq. (44). Here the crucial point is that it is possible to introduce the variable  $\chi(\nu) = \int_0^{\nu} \phi(\nu') d\nu'$ , so that there is no direct dependence on  $\phi$ . However, it is clear that already for  $\phi_{\text{em}} \neq \phi_{\text{abs}}$ , in general  $\Theta^{\text{a}} \neq 1$ , implying that this coordinate transformation can only be achieved approximately, so that the result will depend on the shape of the Lyman  $\alpha$  line. Similarly, in the case  $\phi_{\text{em}} \equiv \phi_{\text{abs}}$ , but for  $\Theta^{\text{a}} \neq 1$  and  $\tau_{\text{abs}} \neq f(z)\chi$ , where  $f(z)$  is a function of redshift only, the result for the escape probability will depend on  $\phi$ . In that case, it will be important how large the deviations from quasi-stationarity are in the range, where most of the contributions to  $P$  originate. If for example the profile is a pure Doppler core, then any photon that is emitted will at most travel, scatter and redshift over a characteristic length  $\Delta\nu/\nu \sim \text{few} \times 10^{-5}$  before escaping. This corresponds to  $\Delta z/z \sim 10^{-5}$ , so that the properties of the medium have not changed very much, and the correction should be  $\Delta N_{\nu}/N_{\nu} \sim \text{few} \times 10^{-3}\%$ . However, if, as in the real problem, radiative transfer is occurring in the distant Lorentz wings, these corrections will be important.

## 4. Corrections to the ionization history

With the results of the previous Section it is possible to estimate the expected changes in the ionization history. In Fig. 11

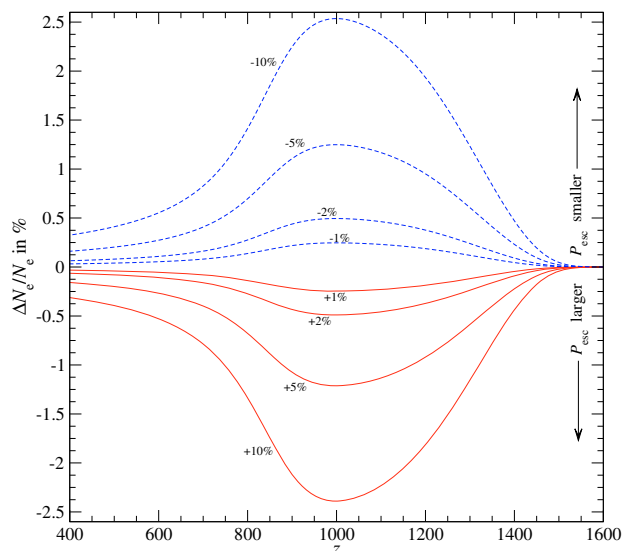


**Fig. 11.** Relative change in the number density of free electrons when allowing for a constant relative change in the Sobolev escape probability of the Lyman  $\alpha$  transition. At maximum  $\Delta N_e/N_e \sim -\frac{1}{4}\Delta P/P$ .

we show how a constant difference in the Sobolev escape probability affects the ionization history. We can see that the response is roughly proportional to the given  $\Delta P/P$ . Therefore we can use the curve for  $\Delta P/P = 1\%$  to estimate the changes in the ionization history for the results given above. Since all the corrections are small, one expects a small additional correction, when computing the escape probability for this modified ionization history. For the purpose of this paper this approximation is sufficient.

Figure 11 also shows that percent level corrections to the escape probability do not affect the ionization history at  $z \gtrsim 1600$ , while at  $z \sim 1000$  one has  $\Delta N_e/N_e \sim -\frac{1}{4}\Delta P/P$ . Also one can see that at low redshifts, changes of the escape probability are not propagating very much to the ionization history, resulting only in  $\Delta N_e/N_e \sim -0.054 \Delta P/P$  at  $z \sim 600$ . Note that the correction of  $N_e$  in both cases is much smaller than the one of the escape probability. This is because the  $2s-1s$  two-photon decay channel already contributes slightly more to the effective recombination rate.

In Fig. 12 we give the correction of the number density of free electrons as a function of redshift. The time-dependent correction of the escape probability leads to a  $\sim 1.6$ – $1.8\%$  change of  $\Delta N_e/N_e$  in the redshift range  $800 \lesssim z \lesssim 1200$ . This change is practically twice as large as the effect due to line recoil (Grachev & Dubrovich 2008), so that the sum of the time-dependent correction and the recoil correction is still dominated by the former contribution, leaving  $\Delta N_e/N_e \sim 0.94\%$  at  $z \sim 1100$ . This will be important for the computation of the CMB power spectra, where at large  $l$  in the case of  $TT$  one expects a  $\Delta C_l/C_l \sim 1\%$ , and about 2 times more for  $EE$ .

## 5. Discussion and conclusions

### 5.1. Main results related to the cosmological ionization history and the CMB power spectra

In this paper we investigated the validity of the Sobolev approximation for the Lyman  $\alpha$  escape probability during hydrogen recombination. We separate absorption and emission of Lyman  $\alpha$  photons from resonant scattering events, including the fact that processes leading to full redistribution of photons over the Voigt

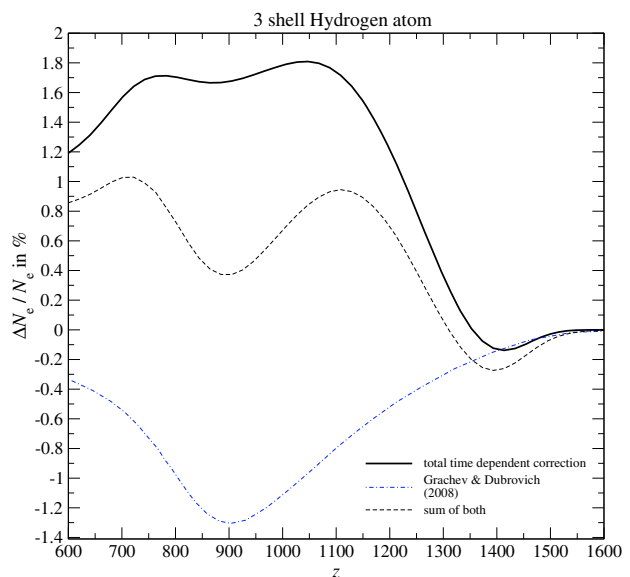


**Fig. 12.** Estimated relative changes in the number density of free electrons when including various physical processes. The curves were obtained by simply multiplying the computed change in the escape probability for the 10 shell case as given in Fig. 9 by the curve in Fig. 11 for  $\Delta P/P = +1\%$  (thick solid line). We also show the result of Grachev & Dubrovich (2008) and the resulting sum of both (dashed).

profile occur with much lower ( $\sim 10^{-3}$ – $10^{-4}$  times) probability than resonant scatterings. We have shown that within the standard formulation the rapid changes in the ionization degree during recombination lead to significant departures of the photon distribution from the quasi-stationary solution. We took these corrections into account analytically, assuming that the photon redistribution process over frequency during a scattering is coherent in the lab frame.

Although one does expect some additional modifications when accounting for partial frequency redistribution, our computations show (Chluba & Sunyaev 2009b) that the additional correction will be dominated by the influence of line recoil, that has been addressed in Grachev & Dubrovich (2008). However, the time-dependent correction that is considered here turns out to be significantly larger, so that we focused on this only. A more complete consideration of this problem is in preparation (Chluba & Sunyaev 2009b).

Here we found that the time-dependent corrections to the effective Lyman  $\alpha$  escape probability result in a  $\sim 1.6$ – $1.8\%$  change of  $\Delta N_e/N_e$  in the redshift range  $800 \lesssim z \lesssim 1200$  (see Sects. 3.4 and 4 for more detail). These corrections are important for the Thomson visibility function and in computations of CMB power spectra, where at large ( $l \sim 1000$ – $3000$ ) multipoles  $l$  in the case of  $TT$  one expects modifications of the order of  $\Delta C_l/C_l \sim 1\%$ , and about 2 times more for  $EE$ . However, note that we also expect additional changes when formulating the problem more rigorously in the two- or multi-photon approach (see discussion in Sect. 5.2).

The main reason for the corrections discussed here are (i) time-dependent changes in the absorption optical depth; and (ii) changes in the net emission rate due to the time-dependence of cosmological recombination. The correction due to case (i) is especially important for contributions coming from the distant wings of the Lyman  $\alpha$  line, where emitted photons can travel, scatter, and redshift over a very long time before getting reabsorbed. For the 3 shell hydrogen atom the associated correction

to the escape probability is  $\Delta P/P \sim -1.2\%$  at  $z \sim 1100$ , while it results in an increase of  $\Delta P/P \sim +2.8\%$  at  $z \sim 1440$  (for more details see Fig. 5).

The correction related to the time dependence of the net emission rate is slightly larger, leading to a total decrease of the effective escape probability at  $z \lesssim 1400$ , that for the 3 shell atom reaches  $\Delta P/P \sim -5.8\%$  at  $z \sim 1140$ , while it results in an increase of  $\Delta P/P \sim +3.7\%$  at  $z \sim 1510$  (for more details see Fig. 8). Here a significant contribution is due to departures of the very distant ( $\sim 10^3$ – $10^4$  Doppler widths) wing spectrum from the quasi-stationary solution (e.g. see Sect. 3.4.5).

We also showed that in particular at low redshifts ( $z \lesssim 800$ – $900$ ) this correction, owing to a self-feedback process, strongly depends on the number of shells that have been taken into account for the computation (see Fig. 9). This is because the effective emission rate depends on the solution for the populations of the excited levels, so that it is important to include at least 4–5 shells into the computations. However, this aspect of the solution appears to be due to the incompleteness in the formulation of the problem, so that at these redshift the conclusions should change when using a two- or multi-photon description (see discussion in Sect. 5.2). Also it is important to mention that for the corrections in the CMB power spectra, this should not affect the results very much.

## 5.2. Apparent problems with the standard formulation

Our analysis shows that under the extreme physical conditions valid in the hot Universe (extremely low plasma density in the presence of the intense CMB radiation field), the standard formulation of the Lyman  $\alpha$  transfer problem leads to several apparently unphysical results. First, we would like to point out that all our computations and estimates clearly show how important (at the percent level accuracy) the distant wings of the lines are for the value the escape probability or mean intensity supporting the 2p level (e.g. see Sects 3.3.4 and 3.4.5). However, in the standard approach variations of the blackbody and also any power-law variations in  $\nu$  are usually neglected in the formulation of the transfer problem and analytic computation, an approximation that is certainly questionable when going to  $|\Delta\nu/\nu| \gtrsim 1\%$ , or  $\sim 10^3$  Doppler width. For example, as we mentioned in Sect. 2.2.4, this approximation leads to a small non-conservation of a blackbody spectrum at large distances from the line center, an aspect that simply follows from exact application of the detailed balance principle, leading to a thermodynamic correction factor  $f = \frac{\nu_2^2}{\nu_1^2} e^{h(\nu-\nu_{21})/kT_\gamma}$ . In a two-photon formulation of the problem this factor automatically appears (Chluba & Sunyaev 2009a).

Also, the emission of photons according to the standard Voigt profile in principle allows the production of photons until arbitrarily large distances on the blue side of the Lyman  $\alpha$  resonance. Without introducing some high frequency cut-off, in the cosmological recombination problem these photons will lead to some unphysical self-feedback at low redshift (e.g. see Sect. 3.4.1), which is also present in our current solution, but at times that are not so important for the CMB power spectra. We expect that both problems can be resolved when using a two- or multi-photon formulation, in which detailed balance is applied self-consistently, and where the line profiles are naturally bound (e.g. see Chluba & Sunyaev 2008) due to energy conservation.

Focusing on the Sobolev approximation (quasi-stationarity of the spectrum and complete redistribution), several unphysical aspects also appear. These are again due to the unique properties

of our Universe, where there are hardly any collision and the expansion rate is so low that the Sobolev optical depth  $\tau_S$  reached values of  $\sim 10^6$ – $10^8$  during recombination. As explained in Sect. 3.2 this leads to the case that the variations of the photon distribution that are important for the mean intensity supporting the 2p level during cosmological recombination occur at distances of  $\sim 10^5$ – $10^8$  Doppler widths from the resonance. This is far beyond the Lyman  $\beta$  line or even the ionization energy of the hydrogen atom.

It is also possible to compute the present day Lyman  $\alpha$  spectral distortion in the time-dependent approach, using the solution 26, for which it was assumed that every line scattering leads to a complete redistribution of photons over frequency. We checked that in this case one would obtain a Lyman  $\alpha$  line profile that is very different from the one computed in the usual  $\delta$  function approximation (e.g. see Rubiño-Martín et al. 2006). One reason for this is that the effective frequency beyond which the photon distribution is no longer affected by the Lyman  $\alpha$  resonance is very far on the red side of the line center (at  $x_D \sim -10^3$  to  $-10^4$ , or  $|\Delta\nu/\nu| \sim 1\%$ – $10\%$ ). This aspect of our computations also suggests that in principle it should be possible to constrain the type of redistribution that is at work during hydrogen recombination by looking at the exact position and shape of the residual Lyman  $\alpha$  distortion in the CMB. In all cases, no line scattering, complete redistribution, and partial redistribution the Lyman  $\alpha$  distortion will look different.

We conclude that for the conditions during cosmological recombination, complete redistribution for a line scattering event in the standard formulation is not an appropriate redistribution process, and leads to rather unphysical results. With the approximation of coherent scattering in the rest-frame, some of the unphysical aspects of the solution disappear. However, as mentioned above, at low redshifts we obtain a large feedback of Lyman  $\alpha$  photons initially released at high redshifts (e.g. see Sect. 3.4.1). These problems can be resolved using a two- or multi-photon formulation.

## 5.3. Future prospects

In spite of all the complications we expect that to lowest order one can take the time-dependent correction during cosmological recombination into account using the solution (49), or in the full two-photon description using a time-dependent solution in the *no-scattering approximation*. Since all additional corrections will (also) be small, one can then compute each other process more or less separately. This should also be possible for the case of helium recombination, but here the reabsorption of photons by the small fraction of neutral hydrogen atoms present at that time will be much more important (Switzer & Hirata 2008a; Kholupenko et al. 2007; Rubiño-Martín et al. 2008).

In order to include the final correction into the computations of the CMB power spectra it will be necessary to develop a fast scheme for the evaluation of the ionization history. For this purpose Fendt et al. (2008) recently proposed a new approach called RICO<sup>13</sup>, which uses multi-dimensional polynomial regression to accurately represent the dependence of the free electron fraction on redshift and the cosmological parameters. Here one first has to produce a grid of models using a given full recombination code, for which each run may take several hours or up to days. However, the time-consuming part of the computation is restricted to the *training* of RICO, while afterwards each call only takes a small fraction of a second. This approach should

<sup>13</sup> <http://cosmos.astro.uiuc.edu/rico/>



allow one to propagate all the corrections in the ionization history that are included in the full recombination code to the CMB power spectra, without using any fudge-factors, like in RECFAST (Seager et al. 1999; Wong et al. 2008). In the future, we plan to provide an updated training set for RICO, including the time-dependent corrections discussed here. This should also make it easier for other groups to cross-validate our results.

*Acknowledgements.* J.C. wishes to thank Dimitrios Giannios, Stefan Hilbert and Stuart Sim for useful discussions. The authors are also very grateful to E. Switzer for carefully reading the manuscript and providing detailed comments. Furthermore the authors would like to thank Prof. Dubrovich, C. Hirata, E. E. Kholupenko, J. A. Rubino-Martin, and W. Y. Wong for very interesting discussions during the workshop “The Physics of Cosmological Recombination” held in Garching, July 2008.

## Appendix A: Computational details

### A.1. Computations of $\phi(\nu)$

The evaluation of the Voigt profile, Eq. (13), is usually rather time-consuming. However, convenient approximations for  $\phi(x_D)$  can be given in the very distant wings and also close to the center of the line. For  $|x_D| \leq 30$  we use the approximation based on the Dawson integral up to sixth order as described in Mihalas (1978, Sect. 9.2, p. 279). In the distant wings of the line ( $|x_D| \geq 30$ ) we apply the Taylor expansion

$$\phi_{\text{wings}} \approx \frac{a}{\pi x_D^2} \left[ 1 + \frac{3 - 2a^2}{2x_D^2} + \frac{15 - 20a^2}{4x_D^4} + \frac{105(1 - 2a^2)}{8x_D^6} \right]. \quad (\text{A.1})$$

We checked that the Voigt function is represented with relative accuracy better than  $10^{-6}$  in the whole range of frequencies and redshifts. Using Eq. (A.1), on the red side of the resonance one can approximate the integral  $\chi = \int_{-\infty}^{x_D} \phi(x') dx'$  by:

$$\chi_{\text{wings}} = -\frac{a}{\pi x_D} \left[ 1 + \frac{3 - 2a^2}{6x_D^2} + \frac{3 - 4a^2}{4x_D^4} + \frac{15(1 - 2a^2)}{8x_D^6} \right], \quad (\text{A.2})$$

as long as  $x \lesssim -30$ . Since  $a \sim 10^{-4} - 10^{-3}$ , this shows that in the distant wings only a very small fraction of photons is emitted. Using the symmetry of the Voigt profile one finds  $\chi(x) = 1 - \chi(-x)$ , such that Eq. (A.2) is also applicable for  $x \gtrsim 30$ .

## References

- Basko, M. M. 1978, *Zhurnal Eksperimental noi i Teoreticheskoi Fiziki*, 75, 1278  
 Chluba, J., & Sunyaev, R. A. 2006a, *A&A*, 458, L29  
 Chluba, J., & Sunyaev, R. A. 2006b, *A&A*, 446, 39  
 Chluba, J., & Sunyaev, R. A. 2007, *A&A*, 475, 109  
 Chluba, J., & Sunyaev, R. A. 2008, *A&A*, 480, 629  
 Chluba, J., & Sunyaev, R. A. 2009a, in preparation  
 Chluba, J., & Sunyaev, R. A. 2009b, in preparation  
 Chluba, J., Rubiño-Martín, J. A., & Sunyaev, R. A. 2007, *MNRAS*, 374, 1310  
 Dubrovich, V. K., & Grachev, S. I. 2005, *Astron. Lett.*, 31, 359  
 Fendt, W. A., Chluba, J., Rubino-Martin, J. A., & Wandelt, B. D. 2008, *ArXiv e-prints*, 807  
 Fixsen, D. J., & Mather, J. C. 2002, *ApJ*, 581, 817  
 Grachev, S. I., & Dubrovich, V. K. 1991, *Astrophysics*, 34, 124  
 Grachev, S. I., & Dubrovich, V. K. 2008, *Astron. Lett.*, 34, 439  
 Hinshaw, G., Nolta, M. R., Bennett, C. L., et al. 2006, *ArXiv Astrophysics e-prints*  
 Hirata, C. M. 2008, *ArXiv e-prints*  
 Hirata, C. M., & Switzer, E. R. 2008, *Phys. Rev. D*, 77, 083007  
 Hummer, D. G. 1962, *MNRAS*, 125, 21  
 Hummer, D. G., & Rybicki, G. B. 1992, *ApJ*, 387, 248  
 Ivanov, V. V. 1973, *Transfer of radiation in spectral lines* (NBS Special Publication, Washington: US Department of Commerce, National Bureau of Standards, English language edition)  
 Kholupenko, E. E., & Ivanchik, A. V. 2006, *Astron. Lett.*, 32, 795  
 Kholupenko, E. E., Ivanchik, A. V., & Varshalovich, D. A. 2007, *MNRAS*, 378, L39  
 Kholupenko, E. E., Ivanchik, A. V., & Varshalovich, D. A. 2008, *ArXiv e-prints*  
 Mihalas, D. 1978, *Stellar atmospheres*, 2nd Ed., (San Francisco: W. H. Freeman and Co.), 650  
 Padmanabhan, T. 2002, *Theoretical Astrophysics, Vol. III: Galaxies and Cosmology* *Theoretical Astrophysics*, by T. Padmanabhan, 638 (Cambridge, UK: Cambridge University Press)  
 Page, L., Hinshaw, G., Komatsu, E., et al. 2006, *ArXiv Astrophysics e-prints*  
 Peebles, P. J. E. 1968, *ApJ*, 153, 1  
 Rubiño-Martín, J. A., Chluba, J., & Sunyaev, R. A. 2006, *MNRAS*, 371, 1939  
 Rubiño-Martín, J. A., Chluba, J., & Sunyaev, R. A. 2008, *A&A*, 485, 377  
 Rybicki, G. B. 2006, *ApJ*, 647, 709  
 Rybicki, G. B., & dell’Antonio, I. P. 1994, *ApJ*, 427, 603  
 Seager, S., Sasselov, D. D., & Scott, D. 1999, *ApJ*, 523, L1  
 Seager, S., Sasselov, D. D., & Scott, D. 2000, *ApJS*, 128, 407  
 Seaton, M. J. 1959, *MNRAS*, 119, 90  
 Seljak, U., Sugiyama, N., White, M., & Zaldarriaga, M. 2003, *Phys. Rev. D*, 68, 083507  
 Sobolev, V. V. 1960, *Moving envelopes of stars* (Cambridge: Harvard University Press)  
 Sunyaev, R. A., & Chluba, J. 2007, *Nuovo Cimento B*, 122, 919  
 Switzer, E. R., & Hirata, C. M. 2008a, *Phys. Rev. D*, 77, 083006  
 Switzer, E. R., & Hirata, C. M. 2008b, *Phys. Rev. D*, 77, 083008  
 Varshalovich, D. A., & Syunyaev, R. A. 1968, *Astrophysics*, 4, 140  
 Wong, W. Y., & Scott, D. 2007, *MNRAS*, 375, 1441  
 Wong, W. Y., Moss, A., & Scott, D. 2008, *MNRAS*, 386, 1023  
 Zeldovich, Y. B., Kurt, V. G., & Syunyaev, R. A. 1968, *Zhurnal Eksperimental noi i Teoreticheskoi Fiziki*, 55, 278